JVI Journals.ASM.org

The Amino-Terminal Domain of Alphavirus Capsid Protein Is Dispensable for Viral Particle Assembly but Regulates RNA Encapsidation through Cooperative Functions of Its Subdomains

Valeria Lulla, Dal Young Kim, Elena I. Frolova, Ilya Frolov

Department of Microbiology, University of Alabama, Birmingham, Alabama, USA

Venezuelan equine encephalitis virus (VEEV) is a pathogenic alphavirus, which circulates in the Central, South, and North Americas, including the United States, and represents a significant public health threat. In recent years, strong progress has been made in understanding the structure of VEEV virions, but the mechanism of their formation has yet to be investigated. In this study, we analyzed the functions of different capsid-specific domains and its amino-terminal subdomains in viral particle formation. Our data demonstrate that VEEV particles can be efficiently formed directly at the plasma membrane without cytoplasmic nucleocapsid preassembly. The entire amino-terminal domain of VEEV capsid protein was found to be dispensable for particle formation. VEEV variants encoding only the capsid's protease domain efficiently produce genome-free VEEV virus-like particles (VLPs), which are very similar in structure to the wild-type virions. The amino-terminal domain of the VEEV capsid protein contains at least four structurally and functionally distinct subdomains, which mediate RNA packaging and the specificity of packaging in particular. The most positively charged subdomain is a negative regulator of the nucleocapsid assembly. The three other subdomains are not required for genome-free VLP formation but are important regulators of RNA packaging. Our data suggest that the positively charged surface of the VEEV capsid-specific protease domain and the very amino-terminal subdomain are also involved in interaction with viral RNA and play important roles in RNA encapsidation. Finally, we show that VEEV variants with mutated capsid acquire compensatory mutations in either capsid or nsP2 genes.

The alphavirus genus in the *Togaviridae* family contains a wide variety of human and animal pathogens (1, 2). Most of the alphaviruses are transmitted by mosquito vectors between vertebrate hosts (3). In mosquitoes, they cause persistent, lifelong infection and do not cause noticeable effects on the biological functions of the vector. In vertebrates, alphavirus infection is characterized by high-titer viremia, which is required for virus transmission to mosquitoes during the next blood meal (4, 5). Many alphaviruses also enter the brain, where they replicate to very high titers and cause severe meningoencephalitis with frequent lethality or neurological sequelae (6).

Venezuelan equine encephalitis virus (VEEV) may represent the most significant public health threat of all alphaviruses (7). It is found in Central, South, and North America, including the United States. It causes periodic, extensive equine epizootics and epidemics of encephalitis with frequent sequelae in humans. It has the potential to be "weaponized" and used by bioterrorists due to its numerous "user-friendly" characteristics. These include, relatively simple large-scale production, high stability, and efficient transmission by aerosol, resulting in severe disease symptoms. In spite of this, no safe, efficient vaccine or therapeutic means have been developed against VEEV infection. The only live experimental vaccine VEEV TC-83 strain was developed more than 4 decades ago by serial passage of the virulent Trinidad donkey strain (8) and has been reported to induce disease-like symptoms in 40% of vaccinees (8–10). Its attenuated phenotype is a result of only two mutations: one in the 5′-untranslated region of the viral genome and the second in the E2 glycoprotein (11). Thus, TC-83 can easily revert to a more pathogenic phenotype (12). Other live attenuated vaccine candidates also demonstrate adverse effects in vaccinees, and their application remains questionable, particularly for immunocompromised individuals. Inactivated viral vaccines are safer than live attenuated viruses but are more expensive, less efficient, and require large-scale production of the virus (10). Subviral particles or virus-like particles (VLPs), produced either *in vitro* or *in vivo*, represent an important alternative to inactivated vaccines (13–15). In contrast to subunit vaccines, they closely mimic the antigenic structure of natural virions and induce a more natural spectrum of neutralizing and protective antibodies but transmit no viral genetic material and are incapable of developing a spreading infection or viremia.

The development of VEEV and other alphavirus VLP-based vaccine candidates requires a detailed knowledge of virion structure, of its assembly and, most importantly, of the mechanism of viral RNA encapsidation. These characteristics have been intensively studied in Sindbis virus (SINV) (16–20) and Semliki Forest virus (SFV) (21–23), which are representative members of the Old World alphaviruses, but our knowledge of VEEV, the most important representative of the New World alphaviruses, remains incomplete. VEEV virions have been analyzed by cryo-electron microscopy (cryo-EM) (24), but there are no data regarding their assembly process.

The VEEV genome encodes four structural proteins, which are translated from the subgenomic RNA, synthesized during virus replication (25). Capsid protein is required for packaging of the viral 11.5-kb RNA genome into nucleocapsid (NC) and also serves

Received 16 July 2013 **Accepted** 29 August 2013
Published ahead of print 4 September 2013
Address correspondence to Ilya Frolov, ivfrolov@UAB.edu.

doi:10.1128/JVI.01960-13

as a self-protease, which mediates the cotranslational cleavage of capsid during structural polyprotein synthesis (2). The downstream E3 glycoprotein is a signal peptide for the E2 glycoprotein and, together with the E2 transmembrane domain, it mediates transport of E2 to the plasma membrane. E3 is eventually cleaved from E2 by a cellular furin protease. The last structural glycoprotein E1 is transported to the plasma membrane as an E2/E1 heterodimer, most likely in the already-assembled trimeric spikes (26). E3 is not a component of the released virions in most alphaviruses, but in VEEV it remains a structural component of the glycoprotein spikes on the surfaces of viral particles (24). The commonly accepted hypothesis regarding alphavirus particle assembly is that NCs are formed in the cytoplasm of infected cells, and this process is mediated by interaction of the capsid protein with the RNA packaging signal (PS), which is present in genomic, but not subgenomic, RNA. The NCs are then transported to the plasma membrane either by themselves or on the surfaces of membranous vesicles, the so-called CPVII, and then bud from the cells while acquiring their lipid envelope with glycoprotein spikes (27, 28). NC itself has an icosahedral geometry and apparently determines the final alphavirus T4 symmetry. Previously published data from SINV and SFV demonstrated the possible existence of an alternative virion assembly mechanism, suggesting that preformation of NCs is not absolutely essential and that NC assembly might proceed at the plasma membrane concomitantly with virion budding (21–22, 29). However, these experiments were performed on capsid deletion mutants exhibiting a low efficiency of particle release, and thus a question was raised about the biological significance of this phenomenon.

Previously, we have shown that VEEV-specific capsid protein could also form NC at the plasma membrane during the virion budding process (30). This process did not require NC preassembly, and in mutants where the positively charged amino acids in the capsid amino terminus were no longer present the released VLPs lacked RNA.

In the present study, we investigated the mechanism of VEEV particle assembly in infected cells in more detail. Our new data reveal an elegant mode of function for VEEV capsid protein in virion assembly. We show that its conserved carboxy-terminal domain is sufficient for particle formation. Expression of this domain and viral glycoproteins leads to VLP formation and release. The amino-terminal domain (amino acids [aa] 1 to 126) of the VEEV capsid protein is generally dispensable for particle formation. However, it contains four subdomains, which have regulatory functions in the particle assembly process and only allow it to proceed if the viral genome is packaged into NC. These subdomains determine the specificity of RNA encapsidation, NC physical stability, and RNA presentation for the encapsidation process.

MATERIALS AND METHODS

Cell cultures. The BHK-21 cells were kindly provided by Paul Olivo (Washington University, St. Louis, MO). They were maintained at 37°C in alpha minimum essential medium (αMEM) supplemented with 10% fetal bovine serum (FBS) and vitamins.

Plasmid constructs. Standard recombinant DNA techniques were applied for plasmid construction. The PCR fragments containing deletions in the capsid gene were cloned into pVEEV/GFP (31) to replace the wild-type (wt) capsid sequence. The resulting plasmids were designated pVEEVΔ1, pVEEVΔ2, pVEEVΔ3, and pVEEVΔ4. Other sets of deletions were performed by using the previously published VEEV/GFP genome with a strongly modified capsid gene, pVEEV/C_{RK4-}/GFP (30), which was designated pVEEV/Cm in the present study to simplify presentation of the data. The resulting plasmids containing corresponding deletions in the modified capsid gene were cloned and are designated pVEEV/CmΔ1, pVEEV/CmΔ2, pVEEV/CmΔ3, pVEEV/CmΔ4, pVEEV/CmΔ23, pVEEV/CmΔ234, pVEEV/CmΔ1234, pVEEV/CmΔ12, pVEEV/CmΔ14, and pVEEV/CmΔ124. The pH/C plasmid, encoding VEEV helper RNA capable of expressing wt VEEV capsid protein, was described elsewhere (30). All of the indicated mutations and the identified adaptive mutations were made by PCR-based mutagenesis. In all of the plasmids, cDNAs of VEEV modified genomes were placed under the control of the SP6 RNA polymerase promoter. They also contained a green fluorescent protein (GFP) gene under the control of a subgenomic promoter. GFP expression was used to monitor virus replication and to measure titers because many of the constructs used were unable to develop plaques or cause a cytopathic effect (CPE). Sequences of the recombinant genomes and details of cloning procedures can be provided upon request.

***In vitro* RNA transcription and electroporation.** Plasmids were purified by centrifugation in CsCl gradients. Before the transcription reaction, plasmids were linearized with MluI. RNAs were synthesized by SP6 RNA polymerase in the presence of a cap analog according to the manufacturer's recommendations (Invitrogen). The yield and integrity of the transcripts were analyzed by gel electrophoresis under nondenaturing conditions. Aliquots of transcription reactions were used for electroporation without additional purification. Electroporation of BHK-21 cells was performed under previously described conditions (32). Many of the rescued mutant viruses were unable to replicate to infectious titers, sufficient to infect cells in the following experiments with a multiplicity of infection (MOI) of >1 infectious unit (inf.u)/cell. Therefore, such defective genomes were packaged into infectious virions with titers $>10^9$ inf.u/ml by coelectroporating their *in vitro*-synthesized RNA and helper RNA genomes. Viral stocks were harvested within 24 h postelectroporation. Titers of plaque-forming viruses were determined by a standard plaque assay on BHK-21 cells (33). The infectious titers of noncytopathic viruses were determined by infecting BHK-21 cells (5×10^5 cells/well) in six-well Costar plates with 10-fold dilutions of the samples and counting the number of GFP-positive cells at 6 h postinfection.

Selection of variants replicating to higher infectious titers. The original stocks of VEEV variants encoding mutated capsids were generated by electroporation of the *in vitro*-synthesized RNA without coelectroporation of RNA helper. Stocks were passaged four times on BHK-21 cells. To select the most efficiently replicating variants, at each passage, we used decreasing volumes of samples harvested at the previous passages for inoculation. Stocks demonstrating more efficient, spreading infection were plaqued on BHK-21 cells, plaque-purified variants were used to infect naive cells, and then RNA was isolated from the cells at 20 h postinfection and used for sequencing of the viral genomes. The identified putative adaptive mutations were cloned back into original constructs, and rescued viruses were additionally tested in terms of rates and titers of the released infectious viruses.

Concentration of viral particles. BHK-21 cells in 150-mm dishes were infected with the designed mutants at an MOI of 20 inf.u/cell for 1 h and then incubated at 37°C in complete, serum-containing media. At 6 h postinfection, the cells were washed three times with serum-free media and further incubated in serum-free VP-SFM medium (Invitrogen). Media were harvested at 20 h postinfection before cells demonstrated a profound CPE, the pH was stabilized by adding HEPES buffer (pH 7.5) to 0.005 M, and possible cell debris was pelleted by centrifugation at 4,500 × *g* for 20 min. Particles were concentrated using centrifugal Ultracel-100K filters (Millipore) at 700 × *g*. In many experiments, particles were also pelleted at 54,000 rpm for 1 h at 4°C in a TLA-55 rotor in a TL-100 tabletop ultracentrifuge (Beckman). Concentrated or pelleted samples were analyzed by SDS-PAGE, followed by either Coomassie blue staining or Western blotting. Western blots were performed using anti-VEEV TC-83 antibodies (a generous gift from R. Tesh [University of Texas Med-

ical Branch at Galveston]), followed by treatment of the membranes with infrared dye-labeled secondary antibodies. Ribosomal proteins were detected using antibody against RPL23 (Sigma) and RPS3 (Cell Signaling Technology), and this was also followed by treatment with infrared dye-labeled secondary antibodies. For quantitative analysis, the membranes were scanned on a LI-COR imager. All of the experiments were highly reproducible and were repeated three to four times. Nevertheless, we always compared only samples produced in the same experiment on exactly the same numbers of cells and purified at the same time.

Fractionation of intracellular nucleocapsids. A total of 2.5×10^6 BHK-21 cells in 100-mm dishes were infected with infectious viral particles containing packaged mutant viral genomes at an MOI of 10 inf.u/cell. These samples were incubated at 37°C for 16 h and then harvested and lysed in phosphate-buffered saline (PBS) containing 10 mM EDTA and 1% Triton X-100. The undissolved material was pelleted at 14,000 rpm for 15 min at 4°C, and then clarified lysates were applied to linear 10 to 50% sucrose gradients prepared with PBS containing 10 mM EDTA. Centrifugation was performed in a SW-40 rotor at 38,000 rpm for 3 h at 4°C. Gradients were fractionated, collected fractions were diluted with PBS, protein complexes were pelleted at 54,000 rpm for 2 h at 4°C in a TLA-55 rotor using a TL-100 tabletop ultracentrifuge (Beckman), and the presence of capsid and ribosomal proteins in the pellets was analyzed by SDS-PAGE, followed by Western blotting. For quantitative analysis, the membranes were scanned on a LI-COR imager.

Electron microscopy. Droplets (3 μl) of virus suspension were placed onto a freshly glow-discharged, 400-mesh copper electron microscope grid covered with a thin carbon film. After ~15 s, the grid was blotted dry, washed with EM buffer (10 mM Tris-HCl [pH 8.0], 20 mM NaCl, 2 mM $MgCl_2$), blotted dry, and then stained for ~30 s using 1% uranyl acetate. Images were acquired at magnification of ×50,000 using a FEI Tecnai F20 electron microscope in the in the UAB cryo-EM core facility.

Quantitative reverse transcription-PCR (RT-qPCR). For analysis of the RNA present in the released particles, samples were pelleted from concentrated stocks corresponding to 6 ml of the harvested media. Samples for RNA analysis also contained 0.1 ml of SINV stock of known concentration. SINV was added prior to centrifugation and used for normalization of the data and to control the quality and reproducibility of RNA isolation. RNA from pelleted samples was isolated using the RNeasy minikit (Qiagen). cDNA was synthesized using equal aliquots of isolated RNA with the QuantiTect reverse transcription kit (Qiagen). Both random and virus-specific reverse primers were used for synthesis. VEEV nsP2- and E1-specific primers were used to quantify genomic and total viral RNAs, respectively. The concentration of β-actin RNA in viral particles was measured by using a pair of β-actin-specific primers. SINV nsP2-specific primers were used to quantify SINV genomic RNA in the samples. Quantitative PCR was performed using SsoFast EvaGreen Supermix (Bio-Rad) in a CFX96 real-time PCR detection system (Bio-Rad) for 40 cycles with two steps per cycle. The specificity of the quantitative PCR was confirmed by analyzing the melting temperatures of the amplified products. The results of quantification were normalized to the amount of SINV RNA in the same sample. The fold difference in RNA concentration was calculated by using the $\Delta\Delta C_T$ method. Each quantitative PCR was performed in triplicate, and the means and standard deviations were calculated.

Analysis of viral RNA synthesis. To analyze the synthesis of virus-specific genomic and subgenomic RNAs, 5×10^5 BHK cells in six-well Costar plates were infected at the same MOI of 20 inf.u/ml, with samples of mutant viral genomes packaged into infectious virions. At 3 h postinfection, the media in the wells were replaced by 0.8 ml of αMEM supplemented with 10% FBS, actinomycin D (1 μg/ml), and [^{3}H]uridine (20 μCi/ml). After 4 h of incubation at 37°C, the total cellular RNAs were isolated by TRizol reagent according to the manufacturer's protocol (Invitrogen), denatured with glyoxal in dimethyl sulfoxide, and then analyzed by agarose gel electrophoresis using previously described conditions (34). Gels were impregnated with 2,5-diphenyloxazole, dried, and autoradiographed.

RESULTS

Deletions of the amino-terminal subdomain SD1, but not SD2, SD3, or SD4, affect genome-free VLP release. In our previous studies, we have designed a number of VEEV variants encoding strongly modified capsid protein, in which the amino-terminal domain had all of the positively charged amino acids replaced by amino acids with no charge (30, 35). These numerous mutations had a deleterious effect on viral genome packaging but, surprisingly, demonstrated only a minor effect on viral particle release and did not noticeably affect the overall three-dimensional structure of the released virions (30). However, upon removal of the lipid envelope by nonionic detergents, the NCs were highly unstable. Fewer than 1 virion per 1,000 contained genomic RNA; therefore, they were termed virus-like particles (VLPs). It was also observed that the preassembled NCs were not present in the infected cells. These data suggested that VEEV virions can be formed very efficiently without preassembly of cytoplasmic NC, and this alternative pathway mediates efficient particle release to high concentrations. In the present study, we initiated a detailed investigation of VEEV egress, focusing on the mechanism of function of VEEV capsid domains in RNA encapsidation and virion formation.

Based on the available structural and functional data of SINV-specific capsid protein, we provisionally divided the amino-terminal domain of VEEV capsid protein into four smaller structural subdomains (SDs) (Fig. 1). (i) SD1 was represented by aa 1 to 37. No functions have been previously assigned to this peptide in either VEEV or other alphaviruses. (ii) The next subdomain, SD2 (aa 38 to 51), was previously predicted to fold into a small alpha helix, helix I. In the case of SINV, helix I was shown to be responsible for dimerization of capsid molecules, required for virus assembly (17). In the case of VEEV, it was demonstrated to function as a nuclear export signal (NES) playing a critical role in inhibition of nuclear pore trafficking (36, 37). In a recent study, we also showed that in VEEV capsid, SD2 was capable of accumulating adaptive mutations (35). These mutations increased the efficiency of VEEV genome packaging by capsid protein mutants by a few orders of magnitude and compensated, to some degree, for the decrease in the capsid's positive charge in these mutants. These adaptive mutations did not generate additional positive charge and functioned synergistically with adaptive mutations accumulating in VEEV nsP2 protein (35). (iii) SD3 (aa 52 to 110) is a highly positively charged subdomain. It appears to mediate most of the RNA-capsid protein binding (19). (iv) SD4 (aa 111 to 126) is the last N-terminal subdomain, which is highly conserved among all of the alphaviruses. In SINV, this subdomain was shown to determine the specificity of viral genome packaging (38) and was proposed to interact with the SINV RNA packaging signal (PS) (39).

The previous data suggested that VEEV NC formation can proceed in the absence of RNA encapsidation (30). To further dissect NC assembly and the roles of SDs in this process, we utilized a VEEV variant (VEEV/Cm), in which the capsid protein gene had all of the codons for positively charged amino acids in the amino terminus mutated (Fig. 1). This experimental system provided us with the opportunity to study NC and particle assembly in the absence of viral RNA packaging and thus to separate the roles of RNA-capsid binding and capsid-capsid interactions in the encap-

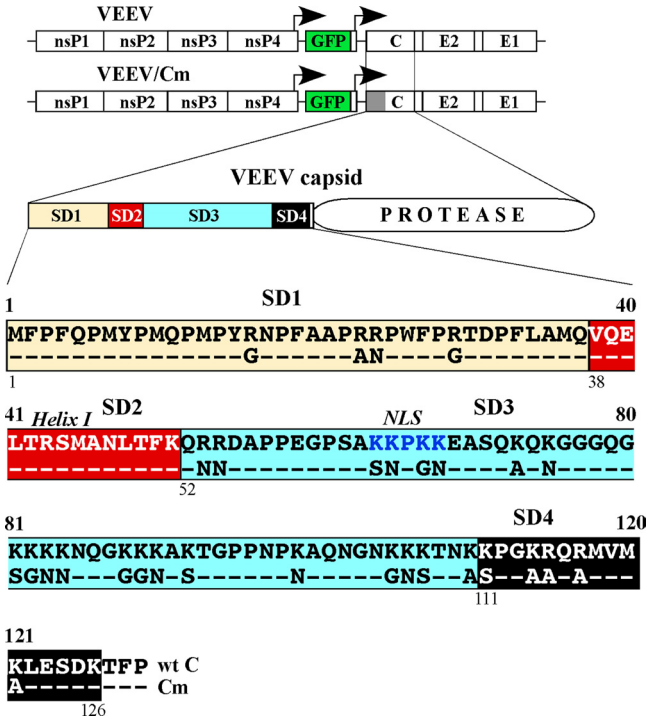

FIG 1 Schematic representation of the originally designed VEEV genomes, encoding wt and mutated capsid proteins, and schematic representation of the domain structure of the capsid protein and sequences of the amino-terminal domains. The amino-terminal subdomains SD1, SD2, SD3, and SD4 are indicated. The sequences of the amino termini of the wt and mutated capsid proteins are aligned, and the introduced mutations are indicated. The arrows above the genome diagrams indicate the positions of the subgenomic promoters.

sidation process. VEEV/Cm also encoded GFP under the control of a second subgenomic promoter. In these and other constructs, its expression was used for evaluation of virus titers and to monitor the spread of infection, since many of the variants were defective in CPE development and spreading.

In the VEEV/Cm-specific capsid gene, we sequentially deleted fragments encoding each of the proposed SDs (Fig. 2A). The defective viral genomes (VEEV/Cm, VEEV/CmΔ1, VEEV/CmΔ2, VEEV/CmΔ3, and VEEV/CmΔ4) were synthesized *in vitro* and coelectroporated into cells with the helper RNA encoding the RNA binding-competent capsid protein (see Materials and Methods for details). All of the genomes were packaged into infectious virions to titers exceeding 10^9 inf.u/ml. These samples were used to infect naive cells at the same MOI, and the released particles were analyzed as described in Materials and Methods.

All of the deletions, other than ΔSD1, had either minor (ΔSD2 and ΔSD4) or no detectable negative effect (ΔSD3) on the amount of released particles. After applying an identical concentration procedure, they were readily detectable by SDS-PAGE, followed by Coomassie blue staining (Fig. 2B), and by quantitative Western blotting (Fig. 2C). Moreover, the deletions did not noticeably affect the sizes of the released VLPs or their overall morphologies (Fig. 2E). However, the deletion of SD1 had a profound effect on particle accumulation in the media. Since the alphavirus capsid-specific SD1 domain was not previously suggested as being critically involved in NC and virion assembly, the most plausible explanation could be, as has been shown for SINV and SFV (40–42), that the VEEV SD1-coding sequence contains a translational enhancer. Therefore, the SD1 deletion mutant was tested in terms of efficiency of structural polyprotein synthesis and accumulation of structural proteins in the infected cells. Cells infected with VEEV/CmΔ1 demonstrated the presence of VEEV glycoproteins at exactly the same level as those found in the cells infected with other mutants (Fig. 2D). We also failed to detect a difference in structural protein synthesis using pulse-labeling of the cells infected with different mutants, with [^{35}S]methionine, followed by SDS-PAGE analysis (data not shown). This was an indication that structural protein synthesis was not affected by the introduced deletion. No degradation products of mutated capsid were detected either. We noticed a lower level of capsid protein in the infected cells using Western blot analyses (Fig. 2D); however, subsequent experiments demonstrated that SD1 contains epitope(s) recognized by the available VEEV-specific antibodies. Thus, capsid proteins, which lacked SD1, always demonstrated lower signals on Western blots (Fig. 2C and D and data not shown). Taken together, the data demonstrated that SD2, SD3, and SD4, but not SD1, were dispensable for particle release, at least in the context of virus with a mutated RNA-binding domain in the capsid protein.

The entire amino-terminal domain of VEEV capsid protein is dispensable for VLP release. The next experiments were aimed at analysis of the effects of more extensive deletions in the amino-terminal domain on particle assembly. The designed variants contained deletions of either two, three, or all four SDs (Fig. 3A). These constructs were also packaged into infectious virions using helper RNA and were used to infect naive cells. In spite of having a large portion the amino-terminal domain or the entire fragment deleted, all of the constructs were capable of efficient VLP release and were readily detectable on Coomassie blue-stained gel (Fig. 3B). Quantitative Western blots demonstrated that deletions of SD2+3+4 or SD1+2+3+4 caused only a 5-fold decrease in VLP formation. These large deletions did not affect the accumulation of viral structural proteins in the cells, and the released particles demonstrated morphologies and sizes similar to those of the VEEV/Cm (Fig. 3E) and wt virus (data not shown). Surprisingly, even the SD1234 deletion mutant produced VLPs, despite retaining only the protease domain of the capsid protein.

There was a noticeable difference in the results of experiments with VEEV/CmΔ1 and VEEV/CmΔ1234 in terms of particle release. In multiple experiments, VEEV/CmΔ1234 was reproducibly more efficient in VLP production than VEEV/CmΔ1, which had a smaller deletion. Therefore, in additional experiments, we compared particle release achieved by VEEV/CmΔ1, VEEV/CmΔ12, VEEV/CmΔ14, VEEV/CmΔ124, and VEEV/CmΔ1234 (Fig. 4A). The results shown in Fig. 4B, exhibiting the Coomassie blue-stained gel, and Fig. 4C, which presents the quantitative Western blot, demonstrate that deletion of SD1 has a strong negative effect on particle formation only in the presence of mutated SD3. As in the previous experiments, this was not a result of different levels of viral structural protein expression (Fig. 4D). Thus, SD3 appears to have a regulatory role in VLP formation/release. The experiments presented in the following sections provide additional experimental support to explain this phenomenon.

The carboxy-terminal, protease domain of VEEV capsid protein can evolve to achieve more efficient RNA packaging. In one of our previous studies, we detected and analyzed the evolution of a VEEV TC-83-based variant, which had numerous mutations

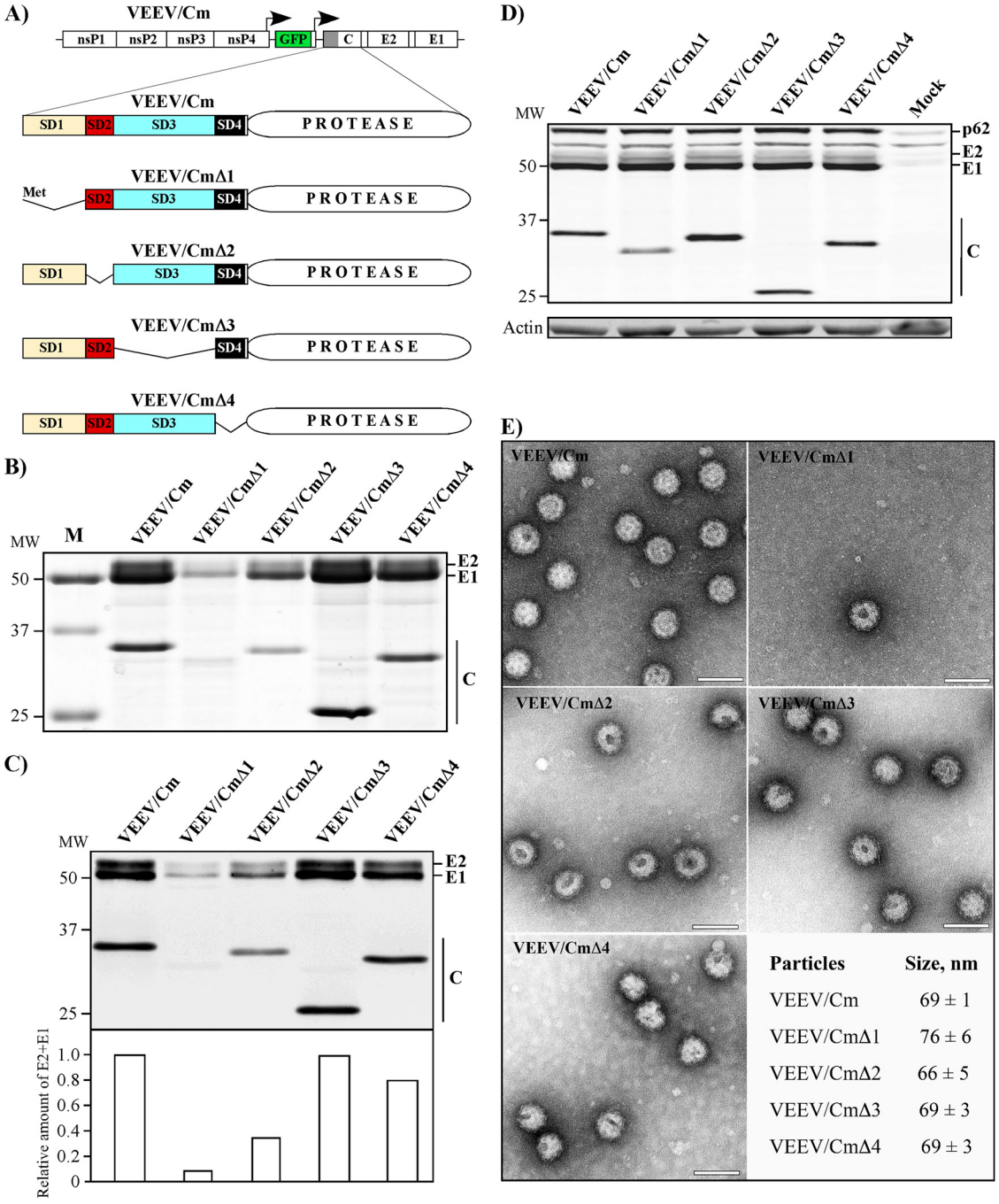

FIG 2 The formation of subviral particles does not depend on the N-terminal SD2, SD3, or SD4, but the deletion of SD1 has a deleterious effect on particle formation. (A) Schematic representation of the VEEV/Cm genome and its variants with sequentially deleted SD1, SD2, SD3, and SD4. (B) Analysis of viral particles released from cells infected at an MOI of 20 inf. u/cell at 20 h postinfection. Particles were collected, concentrated, pelleted, and analyzed by SDS-PAGE as described in Materials and Methods. The gel was stained by Coomassie brilliant blue and represents aliquots corresponding to 2.25 ml of the harvested media. (C) Quantitative analysis of VEEV structural proteins by Western blotting of the samples presented in panel B. The gel contains aliquots corresponding to 0.15 ml of the harvested media. (D) Analysis of viral protein expression in BHK-21 cells infected with the indicated mutants. Cells were infected at an MOI of 20 inf.u/cell and harvested at 8 h postinfection, and the accumulation of virus-specific structural proteins was analyzed by Western blotting with VEEV-specific antibodies. The lower panel represents the same membrane stained with β-actin-specific antibodies. (E) Negative staining and EM analysis of concentrated VLPs released from the cells infected with different mutants (see Materials and Methods for details). The mean sizes of the particles and the standard deviations are presented. Scale bars, 100 nm.

eliminating the positive charge of the amino-terminal domain of capsid protein (35). This variant managed to achieve a goal, which was deemed to be impossible to reach: it evolved in tissue culture and started to produce infectious virus particles a few orders of magnitude more efficiently than the originally designed variant (35). The increase in the ability to package RNA was the result of accumulation of adaptive mutations in SD2 (helix I) and the nsP2-coding gene whose synergistic effects led to increases in infectious titer.

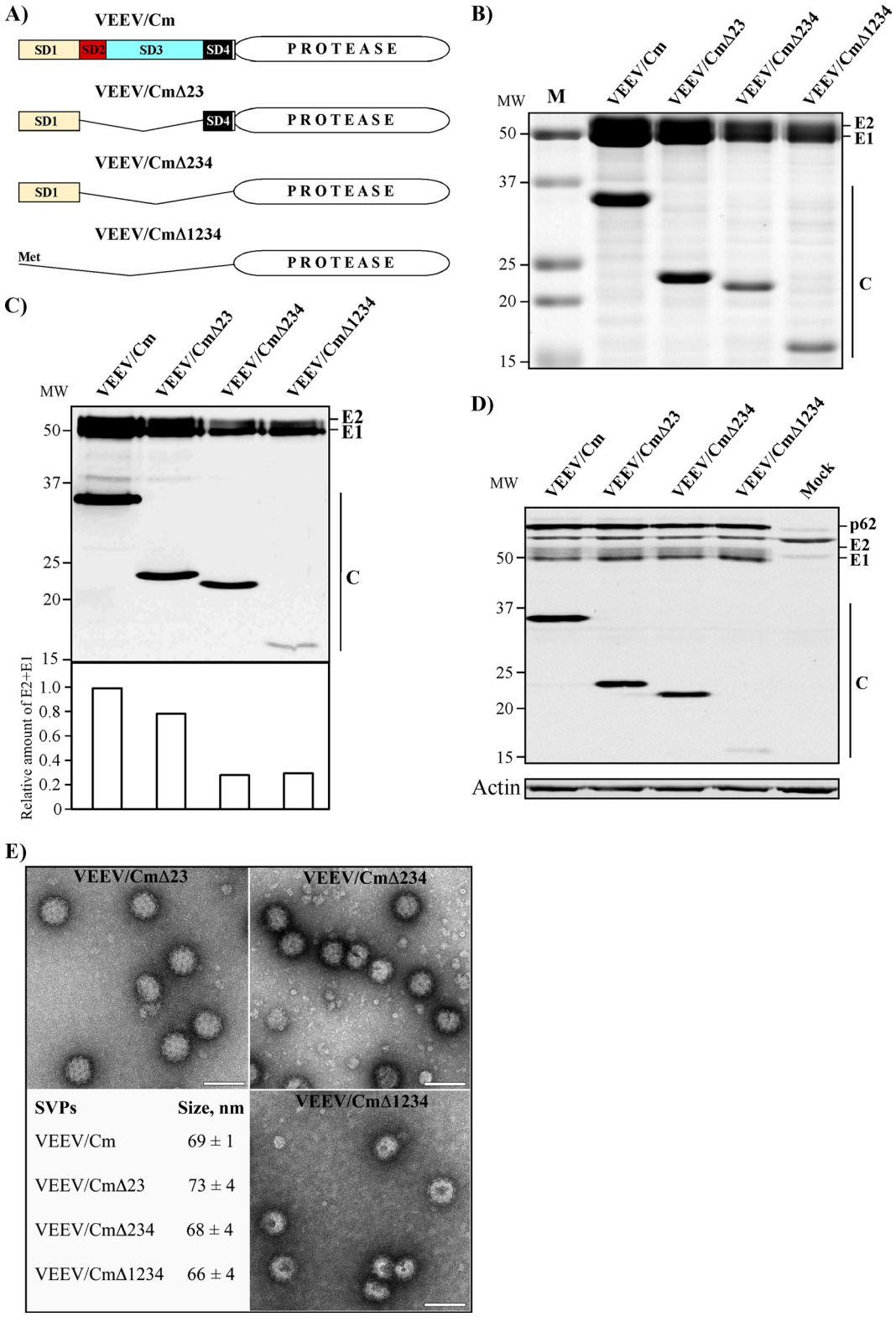

FIG 3 The entire amino-terminal domain of VEEV capsid protein is dispensable for VLP formation. (A) Schematic representation of the VEEV/Cm genome and mutants with multiple subdomains deleted. (B) Analysis of viral particles released from cells infected at an MOI of 20 inf. u/cell at 20 h postinfection. Particles were collected, concentrated, pelleted, and analyzed by SDS-PAGE as described in Materials and Methods. The gel was stained by Coomassie brilliant blue, and aliquots corresponding to 2.25 ml of the harvested media are presented. (C) Quantitative analysis of VEEV structural proteins by Western blotting of the samples presented in panel B. The gel contains aliquots corresponding to 0.15 ml of the harvested media. (D) Analysis of viral protein expression in BHK-21 cells infected with the indicated mutants. Cells were infected at an MOI of 20 inf.u/cell and harvested at 8 h postinfection, and the accumulation of virus-specific structural proteins was analyzed by Western blotting with VEEV-specific antibodies. (E) Negative staining and EM analysis of concentrated VLPs released from cells infected with different mutants (see Materials and Methods for details). The mean sizes of the particles and the standard deviations are presented. Scale bars, 100 nm.

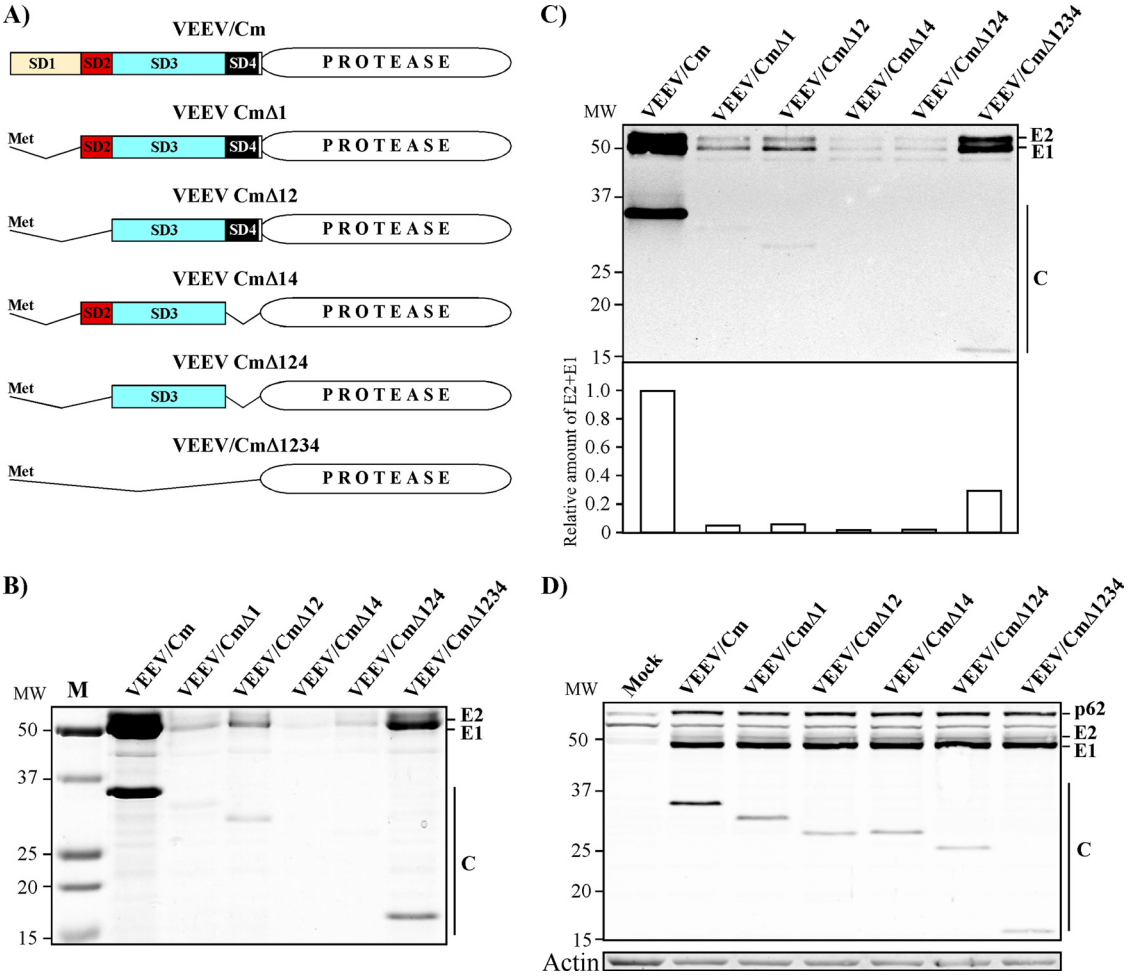

FIG 4 SD1 plays a critical role in VLP formation in the presence of SD3 in the amino-terminal domain of capsid protein. (A) Schematic representation of the VEEV/Cm genome and its variants containing different combinations of SD deletions. (B) Analysis of viral particles released from cells infected at an MOI of 20 inf. u/cell at 20 h postinfection. Particles were collected, concentrated, pelleted, and analyzed by SDS-PAGE as described in Materials and Methods. The gel was stained by Coomassie brilliant blue and displays aliquots corresponding to 2.25 ml of the harvested media. (C) Quantitative analysis of VEEV structural proteins by Western blotting in the samples presented in panel B. The gel contains aliquots corresponding to 0.15 ml of the harvested media. (D) Analysis of viral protein expression in BHK-21 cells infected with the indicated mutants. Cells were infected at an MOI of 20 inf.u/cell and harvested at 8 h postinfection, and the accumulation of virus-specific structural proteins was analyzed by Western blotting with VEEV-specific antibodies.

All of the newly designed deletion mutants, containing either one or more SDs deleted, were passaged in BHK-21 cells; however, only VEEV/CmΔ3 and VEEV/CmΔ23 evolved variants capable of developing a spreading infection. Independent stocks of VEEV/CmΔ23 repeatedly acquired the same mutation G262R (the numeration of amino acids corresponds to the wt capsid protein) and, as in the previously described evolution of capsid protein containing intact SD2, VEEV/CmΔ3 also acquired mutations both in the capsid-coding sequence and in nsP2. Further selection experiments with VEEV/CmΔ3 showed that replicating variants contained mutations in two proteins—V555M or N75L mutations in nsP2 and G262R or E194K mutations in capsid protein, respectively. Cloning of these mutations into the originally designed constructs confirmed their positive effect on RNA encapsidation. The G262R mutation increased the rates of infectious VEEV/CmΔ3 and VEEV/CmΔ23 release. The final titers were 10- to 50-fold higher than those of the original constructs, and thus the viruses became capable of developing spreading infection. Surprisingly, they also became more cytopathic. The capsid-specific mutations were modeled into known structure of VEEV capsid (PDB 3J0C). Surprisingly, both of them were closely located on the surface of the protease domain of capsid protein, which is exposed to RNA. Moreover, both mutations led to an increase of basic charge of this surface (Fig. 5). According to the crystal structure, this surface already contains a strong positive charge, and the identified mutations led to its additional increase, which lends further support to the perceived importance of the carboxy-terminal protease domain in RNA binding.

Taken together, these results strongly suggest that the amino-terminal domain of VEEV capsid protein is not essential for particle assembly; the glycoproteins and the carboxy-terminal protease domain of the capsid are capable of efficient VLP formation. This is a clear indication that VEEV particles can be efficiently formed due to protein-protein interactions in the absence of RNA binding.

The amino-terminal domain of capsid protein is a regulator of infectious virion assembly. The experiments described in the

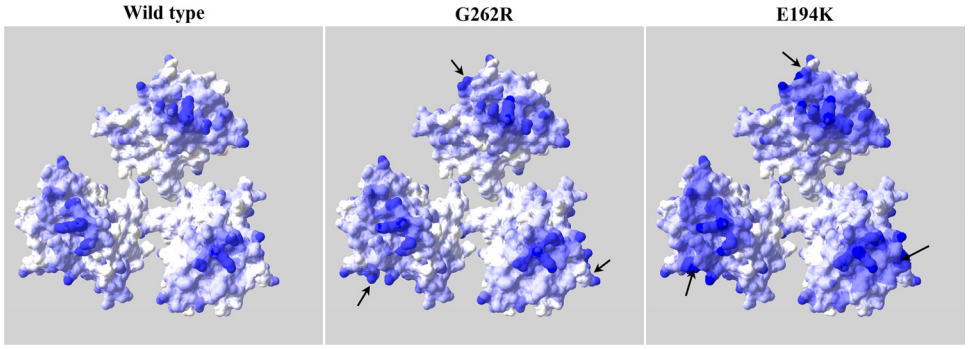

FIG 5 Adaptive mutations in VEEV/CmΔ3 increase the positive charge of the capsid surface exposed to the RNA core. The three copies of capsid were extracted from PDB 3J0C structure. The view is from the inside of the RNA core of the nucleocapsid. The positions of the acquired mutations are marked by arrows. The electrostatic potential surface is drawn with limits of ±10 kT/e.

previous section demonstrated that VEEV RNA and the capsid's amino terminus are dispensable for virion formation. However, thus far there are no data showing that particles released from wt VEEV-infected cells contain a detectable concentration of RNA-free virions. This suggests that either RNA packaging is an incredibly efficient process, or the amino-terminal domain is a negative regulator of particle formation unless it is bound to RNA. To experimentally test these possibilities, we introduced capsid protein-RNA interactions back into the experimental system and investigated their roles in infectious particle release. The experiments were performed in the context of VEEV TC-83, which encoded a wt capsid gene with a natural, positively charged amino-terminal domain. Thus, it was fully capable of packaging viral genome. As in the above sections, the individual SDs were sequentially deleted (Fig. 6A) from the VEEV TC-83 genomes, and the *in vitro*-synthesized RNAs were transfected into BHK-21 cells. All of the introduced deletions had negative effects on infectious titers and, at 24 h postelectroporation, these titers remained too low to perform any further experiments, requiring infection of the cell monolayer with an MOI higher than 1. Therefore, the defective genomes were packaged into infectious virions using helper, wt capsid-producing RNA. All of the generated stocks had titers of $>10^9$ inf.u/ml, and they were used in the following experiments.

BHK-21 cells were infected with the packaged deletion mutants at an MOI of 20 inf.u/cell, and infectious virus titers were assessed at different times postinfection (Fig. 6B). All of the deletions resulted in a profound decrease in infectious virus release, suggesting that all of the SDs—SD1, SD2, SD3, and SD4—play important roles in RNA packaging. However, decreases in infectious titers do not necessarily mean that particles are formed inefficiently. Therefore, in the next experiments, we analyzed concentrations of the released particles at 24 h postinfection of BHK-21 cells (see Materials and Methods for details). The deletions had no effect on synthesis of viral structural proteins (Fig. 6C), but most of them, except Δ3, had a deleterious effect on particle formation (Fig. 6D). The variant with deleted SD3 produced viral particles at a level comparable to that of wt VEEV TC-83, but the infectious titers were lower (Fig. 6B and D). The most plausible explanations for these data are that (i) a high positive charge of SD3 prevents RNA-free NC formation, and SD3 functions as a negative regulator of VLP formation, unless its positive charge is neutralized by bound RNA, and that (ii) deletions of any other subdomains have strong negative effects on the ability of SD3 to interact with viral and possibly other RNAs and thus alter the neutralization of the SD3's positive charge and VLP release. In support of this, the data presented in Fig. 6E demonstrate that, indeed, the deletions of SD1, SD2, or SD4 lead to efficient packaging of cellular mRNAs (right panel) and the deletions of SD4 or SD3 result in efficient packaging of subgenomic rather than genomic RNA (left panel). Another interesting effect was the noticeable decrease of PFU/genome equivalent (GE) ratio demonstrated by the mutants (central panel). This result is indicative of lower infectivity of particles, but since numerous explanations are possible for this effect, we chose not to investigate it further.

VEEV with deletions of individual SDs in capsid protein adapt and replicate to high infectious titers. Alphaviruses and other viruses with RNA genomes of positive polarity demonstrate high level of adaptation to mutations introduced into their nonstructural and structural proteins. They are able to acquire second site mutations, which compensate for the introduced defects, and these adaptive mutations often generate important information about protein-protein and protein-RNA interactions. Therefore, inefficiently replicating VEEV variants, which had deletions of individual SDs and rescued without using helper RNA, were passaged three to five times in BHK-21 cells to test the possibility of their evolution to higher infectious titers. VEEV Δ2, VEEV Δ3, and VEEV Δ4, but not VEEV Δ1, developed variants producing a few orders of magnitude higher infectious titers. We randomly selected two plaques for each adapted variant and sequenced capsid-, nsP2-, nsP3-, and packaging signal-coding sequences in their genomes. The identified mutations were consequently cloned back into the original variants and tested in terms of their positive effect on the rates of virus replication and infectious titers.

The ability of VEEV encoding Cm, the capsid protein lacking the positive charge in the amino-terminal domain, to form virions without NC preassembly certainly cannot be considered conclusive evidence that plasma membrane is the only location of particle formation. In wt alphavirus-infected cells, cytoplasmic NCs are formed, and it is unlikely that they are not later involved in virion formation. Therefore, in the following experiments, besides other characteristics, we studied the preformation of cytoplasmic NCs using the originally designed viral mutants and their adapted variants. Infected cells were treated with nonionic detergent, and the NCs were analyzed by ultracentrifugation in sucrose density gradients. In the same experiment, we compared the NC levels in infected cells and infectious virus release. Figure 7A presents the

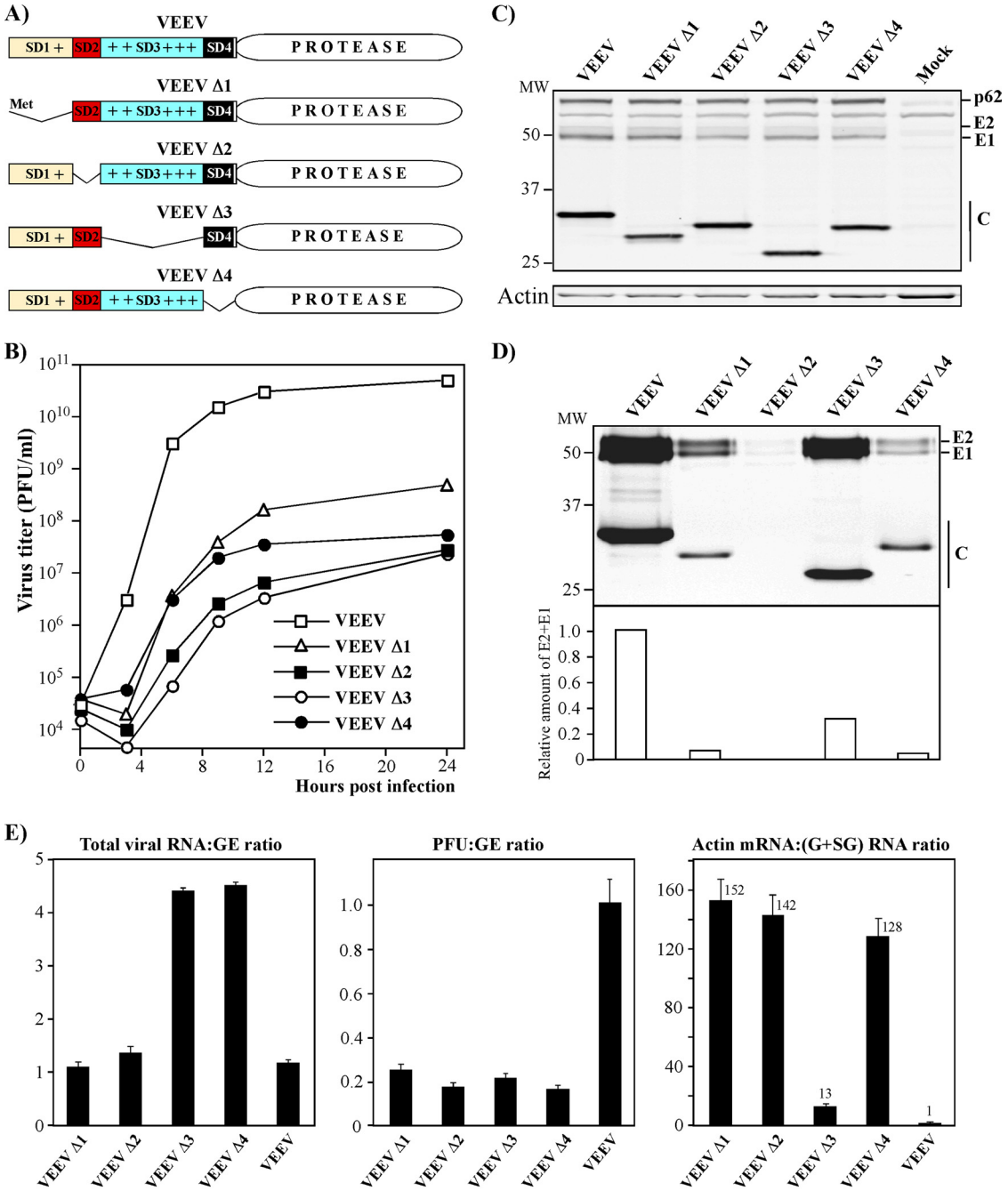

FIG 6 All of the SDs in the amino terminus of wt VEEV capsid protein play critical roles in packaging of viral genome and infectious virus release. (A) Schematic representation of the wt VEEV capsid protein and its variants with deleted amino-terminal subdomains. (B) A total of 5×10^5 BHK-21 cells in 35-mm dishes were infected with VEEV/GFP and mutated genome-containing particles at an MOI of 20 inf.u/cell. Media were replaced at the indicated times postinfection, and the infectious titers were determined as described in Materials and Methods. (C) Analysis of viral protein expression in BHK-21 cells infected with the indicated mutants. Cells were infected at an MOI of 20 inf.u/cell harvested at 8 h postinfection, and the accumulation of virus-specific structural proteins was analyzed by Western blotting with VEEV-specific antibodies. (D) Quantitative analysis of VEEV structural proteins by Western blotting. The gel contains aliquots corresponding to 0.15 ml of the harvested media. (E) Comparative analysis of total viral RNA, genomic RNA, and actin RNA ratios in the released viral particles were determined by RT-qPCR. GE, genome equivalent.

results of an analysis of the control NC samples isolated from virions and cells infected with VEEV TC-83. It also shows the position of capsid protein bound to the ribosomes, whose location in the gradient was analyzed using specific antibodies. Importantly, no NCs were detected in another control, VEEV/Cm-infected cells, and no capsid was associated with ribosomes (Fig. 7A).

(i) VEEV Δ1 variant. The VEEV Δ1 variant demonstrated no evolution toward higher infectious titers or the formation of larger plaques. This was the only subdomain whose function apparently could not be compensated for by acquiring adaptive mutations. VEEV Δ1 was completely incapable of forming intracellular NCs and replicated to titers 100-fold lower than those of the wt virus.

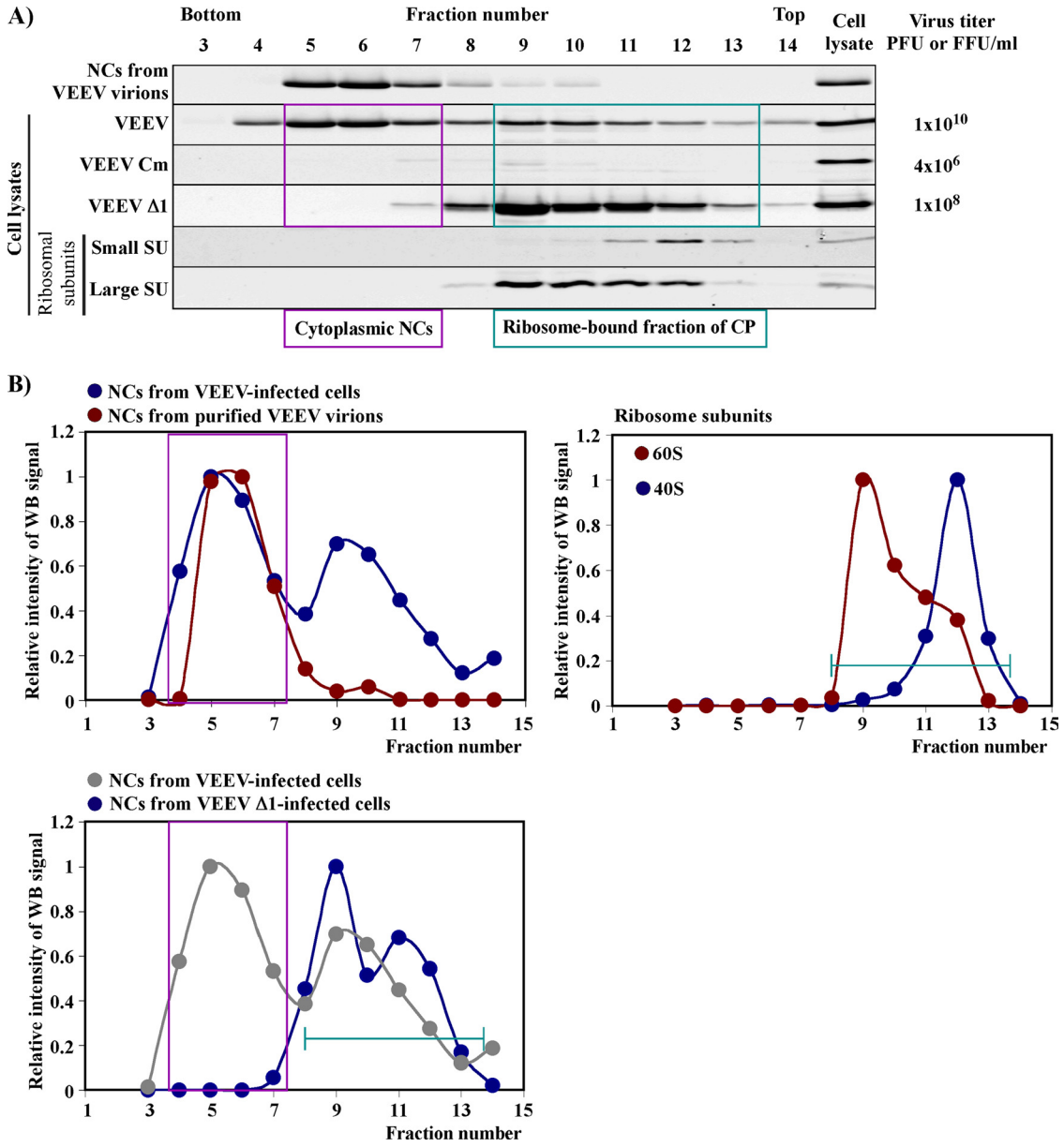

FIG 7 Deletion of SD1 in wt capsid protein has a deleterious effect on the accumulation of NCs in the infected cells. (A) Results of one of the reproducible analyses of NC and capsid protein distribution in sucrose gradients. Cells were infected and lysed as described in Materials and Methods. The details of ultracentrifugation, fractionation of the gradients, and analysis of fractions by Western blotting were performed according to the protocols presented in detail in Materials and Methods. Titers of the released viruses were determined at the time of cell harvesting, at 16 h postinfection. The same membranes were stained with antibodies specific to ribosomal proteins, and two representative blots are presented. (B) Results of quantitative analysis of capsid and ribosomal protein distribution in various fractions in panel A. In each gradient, values were normalized to the signal detected in the fraction with the highest concentration of capsid protein. Pink boxes indicate the distribution of cytoplasmic NCs. Green lines indicate positions of the ribosome-bound fraction of capsid proteins.

(ii) VEEV Δ2 variant. The selected VEEV Δ2 variant producing higher infectious titers contained a single point mutation, K64E (the numbering corresponds to the wt capsid), in the capsid-coding sequence (Fig. 8A), and cloning of this mutation back into the original construct confirmed its stimulatory effect on infectious virus release (Fig. 8A and D). Comparative analysis of NC accumulation in the cells infected with VEEV Δ2 and its adapted variant VEEV Δ2ad demonstrated that the identified mutation caused a strong increase in accumulation of preformed NC (Fig. 8B and C), which could result in higher infectious titers. The identified mutation was in an interesting position, in the capsid-specific NLS (36, 37). SD2 has a common function in the alphaviruses in assembly of NC, but in VEEV it also functions as an NES (36, 37), required for blocking the nuclear pores. Therefore, as we have demonstrated in our previous extensive studies (43, 44), deletion of NES likely led to a higher level of VEEV capsid accumulation in the nuclei and thus made it incapable of forming NC. On the other hand, the indicated K64E mutation also added a negative charge to the highly positively charged capsid, and this could lead to more efficient electrostatic interaction between the capsid molecules.

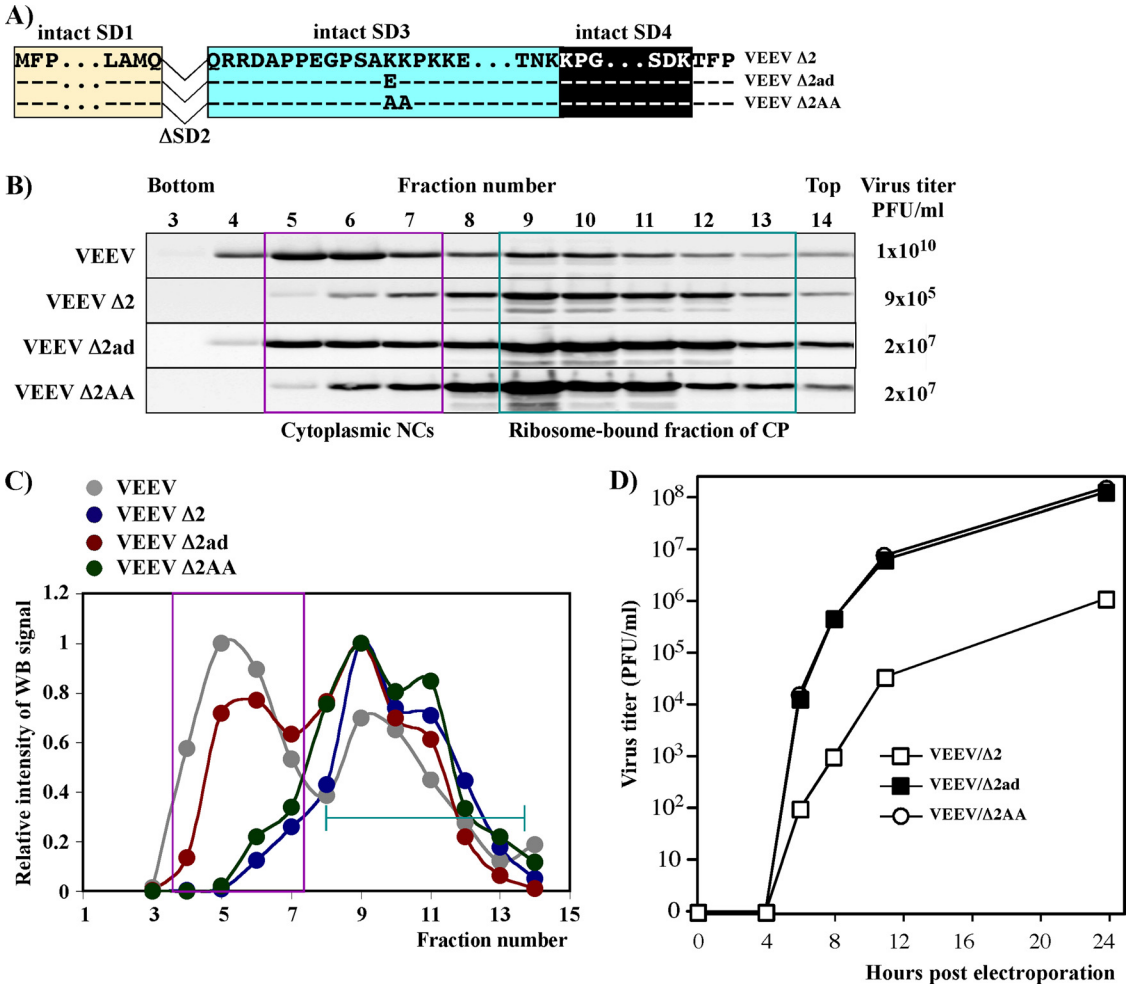

FIG 8 Mutations in the capsid protein-specific NLS compensate for the deletion of SD2 and increase the infectious titers of the VEEV Δ2 mutant. (A) Schematic alignment of the amino-terminal domain of the originally designed capsid protein of VEEV, the VEEVΔ2 mutant, the adapted variant VEEV Δ2ad, and the mutant containing a double mutation introduced into the NLS (VEEV Δ2AA). (B) Results of one of the reproducible analyses of NC and capsid protein distribution in sucrose gradients. Virus titers were determined at the time of cell harvesting at 16 h postinfection. (C) Results of quantitative analysis of the capsid and ribosomal protein distribution in the fractions presented in panel B. In each gradient, the values were normalized to the signal detected in the fraction with the highest concentration of capsid protein. Pink boxes indicate the distribution of cytoplasmic NCs. Green lines indicate the positions of the ribosome-bound fraction of capsid proteins. (D) Comparative analysis of the infectious virus release by the originally designed mutant and its adapted variant. BHK-21 cells were electroporated with 4 μg of *in vitro*-synthesized RNA of VEEV Δ2, VEEV Δ2ad, and VEEV Δ2AA. Media were replaced at the indicated time points, and infectious titers of released viral particles were determined as described in Materials and Methods.

To distinguish between these two possibilities, we designed an additional mutant. It contained a double mutation K64A+K65A in the NLS (VEEV Δ2AA) (Fig. 8A). It also demonstrated a strong positive effect on infectious virus titers (Fig. 8C), suggesting inactivation of the NLS rather than an additional negative charge determined the increase in infectious titer. However, it should be noted that adapted variants still demonstrated replication rates and final titers >10-fold lower than those of the wt virus. Importantly, in repeated experiments, the increase in the rates of infectious VEEV Δ2AA release did not correlate with the intracellular NC accumulation. This finding was suggestive that another, NC-preassembly-independent, mechanism of particle formation is involved.

(iii) VEEV Δ3 variant. The VEEV Δ3 variant, containing a deletion of the positively charged subdomain SD3 (Fig. 9A), had an interesting phenotype. Upon delivery into the cells, it produced capsid protein, which was still able to make large intracellular complexes, which sedimented similarly to the wt NCs in sucrose gradients (Fig. 9B). Cells efficiently released VLPs (Fig. 6D), and infectious titers were always 3 to 4 orders of magnitude lower than those of wt VEEV (Fig. 6B and 9A). Thus, large capsid-containing complexes, apparently formed in the cells without RNA, based on the interactions of the residual SDs. Next, VEEV Δ3 rearranged its capsid gene to restore the protein's positive charge. This was achieved by duplicating a part of SD2-coding and the entire SD4-coding sequences in the originally designed mutated capsid gene. This duplication led to the appearance of 11 additional positively charged amino acids in SD3 (producing 13 instead of the wt 21), which appeared to be sufficient for better RNA binding (Fig. 9A) and made it capable of packaging viral genomes to >100-fold-higher infectious titers. However, we cannot rule out the additional possibility that the duplicated SD4 might have a positive

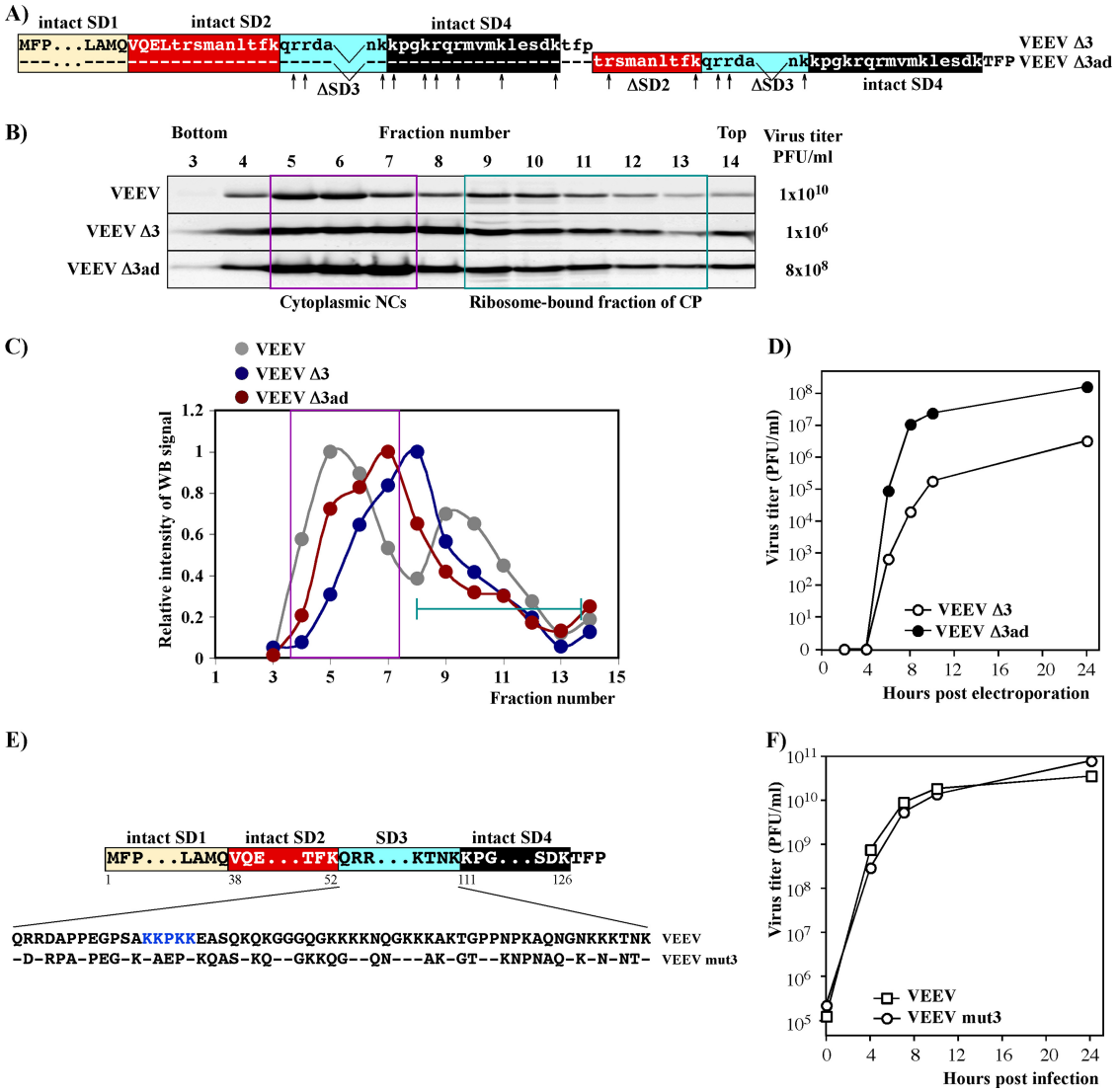

FIG 9 The reduction in infectious titers caused by the deletion of SD3 in VEEV capsid protein can be compensated for by acquiring nonspecific peptides with high positive charges. (A) Schematic alignment of the amino-terminal domain of VEEV capsid protein SD3 deletion mutant and the selected adapted mutant, which replicates to higher infectious titers (VEEV Δ3ad). Black arrows indicate positively charged amino acids in the new SD3 fragment. (B) Results of one of the reproducible analyses of NC and capsid protein distribution in sucrose gradients. Virus titers were determined at the time of cell harvesting at 16 h postinfection. (C) Results of quantitative analysis of the Western blot membranes presented in panel B. In each gradient, the values were normalized to the signal detected in the fraction with the highest concentration of capsid protein. Pink boxes indicate the distribution of cytoplasmic NCs. Green lines indicate the positions of the ribosome-bound fraction of capsid proteins. (D) Comparative analysis of the infectious virus release by the originally designed mutant and its adapted variant. BHK-21 cells were electroporated with 4 μg of *in vitro*-synthesized RNA of VEEV Δ3 and VEEV Δ3ad. Media were replaced at the indicated time points, and titers of infectious viral particles were determined as described in Materials and Methods. (E) Alignment of the SD3-specific amino acid sequences in wt SD3 and SD3 with randomized amino acid sequence in VEEV mut3. (F) Comparative analysis of infectious virus release by the originally designed mutant and its adapted variant. Subconfluent BHK-21 cells in 35-mm dishes were infected with VEEV or VEEV mut3, generated by electroporation of genomes into BHK-21 cells, at an MOI of 20 PFU/cell. Media were replaced at the indicated times postinfection, and infectious titers were determined as described in Materials and Methods.

effect on RNA packaging. Interestingly, the dramatic increase in infectious titers did not correlate with changes of distribution of the capsid-containing protein complexes in sucrose gradients, suggesting that the formation of stable genome-containing NCs in the cytoplasm remained low. Based on the available data, we speculate that the originally designed VEEV Δ3 mutant preferentially encapsidated viral subgenomic RNA (Fig. 6F), which has a length sufficient to neutralize the reduced positive charge of the NC. However, the evolved capsid protein required larger, genomic RNA to neutralize the charge introduced by the newly evolved Arg and Lys in the NC. This strongly increased the frequency of genomic RNA encapsidation (Fig. 9D). Importantly, this evolved capsid protein demonstrated a positive effect on the synthesis of viral genomes (Fig. 11), and this could be an additional contribution to more efficient genome packaging.

The new positively charged domain acquired during VEEV Δ3 evolution was very different from the natural wt sequence. This was suggestive that the latter domain's function may be indepen-

dent of the amino acid sequence and simply requires a sufficient number of positively charged amino acids. To test this possibility, we designed an artificial SD3 in the context of the wt VEEV TC-83 genome. It had the same number of positively charged amino acids as the wt, but these and other amino acids were positioned differently (Fig. 9E). It spite of this extensive mutagenesis, the designed VEEV mut3 replicated at exactly the same rates in terms of infectious virus release (Fig. 9F), suggesting that the function of the SD3 is independent of the amino acid sequence.

(iv) VEEV Δ4 variant. The VEEV variant containing the SD4 deletion used a different means to evolve to higher infectious titers. During passaging in BHK-21 cells, it acquired adaptive mutations in the nsP2-coding sequence but not in the capsid gene (Fig. 10A). The adaptive mutations induced a more efficient accumulation of intracellular NCs (Fig. 10B and C) and increased plaque size and virus replication rates (Fig. 10D and E). They also had a positive effect on RNA replication (Fig. 10F and 11). However, it remains unclear whether the detected 6- to 7-fold differences in RNA replication directly resulted in the dramatic increase in NC formation and infectious virus release or whether the mutated nsP2 itself had an additional positive effect on RNA encapsidation. In any case, this result was in agreement with our previous study, which showed that the inability of VEEV capsid to package viral RNA could be compensated for by adaptive mutations in viral nonstructural protein nsP2.

DISCUSSION

In recent years, great progress has been made in the understanding of alphavirus virion structure (24, 45, 46). The results of crystallization of the individual proteins and their complexes were complemented by cryo-EM-based studies of viral particles, which have provided the field with a detailed knowledge of the structures of alphavirus glycoprotein spikes and their interactions with NC. However, the particle assembly process and the NC assembly in particular remain poorly understood. The primary thesis of the currently prevailing assembly model is that alphavirus nucleocapsids are formed in the cytoplasm, mostly at the sites of viral RNA replication, and then are transported to the virion budding sites at the plasma membrane. This hypothesis relies heavily on the previously published data, which showed that replication of viral RNA proceeds in membrane spherules, which accumulate on the surfaces of lysosomes and modified late endosomes (47). According to this scenario, the newly synthesized viral genomes, which are released by the spherule-located replication complexes, are encapsidated and then delivered to the plasma membrane on the surface of CPV II vesicles and probably through a passive diffusion process. The experimental data support this possibility: alphavirus nucleocapsids accumulate in the cytoplasm (22) (Fig. 7), and the published data suggest that upon delivery to the plasma membrane, even *in vitro*-preassembled nucleocapsid-like complexes can acquire the envelope (48). However, in the last few years, our understanding of the alphavirus RNA replication mechanism has undergone some modifications. It was demonstrated that for some of the alphaviruses, such as SINV and VEEV, replication complexes are formed at the plasma membrane, and a major fraction of them remain there, even at later stages of the infection and continue to function as sites of viral RNA synthesis (49–51). Thus, RNA replication and its packaging into virions are likely to be more closely compartmentalized than we previously thought. NC preassembly may therefore not be an absolutely essential step in viral particle formation. This possibility was also suggested by previous studies of replicating SFV and SINV mutants with large deletions in the capsid protein (19, 21, 22, 29). These mutants formed particles without detectable NC preformation in the cytoplasm, and this was suggestive of the existence of another mechanism of virion release—a mechanism in which NC and virion assembly proceed at the same time. Moreover, it was demonstrated for SFV and CHIKV that structural proteins are able to assemble into VLPs in the absence of genomic RNA (52). In addition, it has been recently shown for SINV that newly synthesized capsid protein-recruiting and E2 protein-containing dynamic structures are detectable at the PM, indicating their possible role in virus assembly and egress (53).

The results of this new study suggest that in the case of VEEV, this NC preassembly-independent mechanism also functions. It is difficult to conclusively detect it in wt virus-infected cells, which contain high concentration of already assembled NCs. However, this NC preassembly-independent mechanism can be easily dissected using VEEV variants expressing mutant capsid proteins, which are incapable of forming stable NC. Cells infected with such VEEV mutants, release viral particles with efficiency comparable to that of the wt virus, suggesting that the second mechanism of particle formation is very productive.

In the present study, we used this alternative pathway of VEEV particle formation to further dissect the molecular mechanism of their assembly and define the function of different capsid-specific amino acid sequences in orchestrating this process. The entire amino-terminal domain of VEEV capsid was found to be dispensable for particle formation and release (Fig. 3). Cells infected with VEEV variants encoding VEEV glycoproteins and only the protease domain of capsid protein produced very high levels of genome-free virions. Thus, interactions between glycoprotein spikes and capsid molecules were sufficient for the assembly process.

The amino-terminal, positively charged domain of the VEEV capsid protein was in turn found to express a number of regulatory and structural functions, aimed to mediate selective packaging of viral genome and to avoid release of particles lacking the viral genome or containing heterologous genetic material. The distinct small subdomains in the capsid's amino terminus accomplished multiple levels of control to achieve the release of genome-containing virions.

The most positively charged capsid-specific subdomain (termed here SD3) contains 21 Arg and Lys amino acids and functions as an efficient negative regulator in the virion assembly process. Deletion of this domain or mutation of all of its positively charged amino acids results in the high-level release of genome-free VLPs. A VEEV mutant, lacking SD3 in the capsid protein but retaining the other SDs, efficiently forms large complexes in the infected cells (Fig. 9). However, they sediment more slowly than wt NCs, and the majority of the resultant viral particles lack viral genomes.

In wt virus-infected cells, the high positive charge of natural SD3 is neutralized by bound viral RNAs. Based on the presented data, this RNA-binding function does not depend on the SD3-specific aa sequence but is determined entirely by a high number of positively charged amino acids. At first glance, it seems that they can be easily neutralized by any other RNA species contained in the cell. However, this does not appear to be the case. In the absence of either SD1, SD4, or SD2 in particular, virions become capable of packaging other RNAs (Fig. 6E), indicating that they can nonspecifically neutralize SD3, but particle production re-

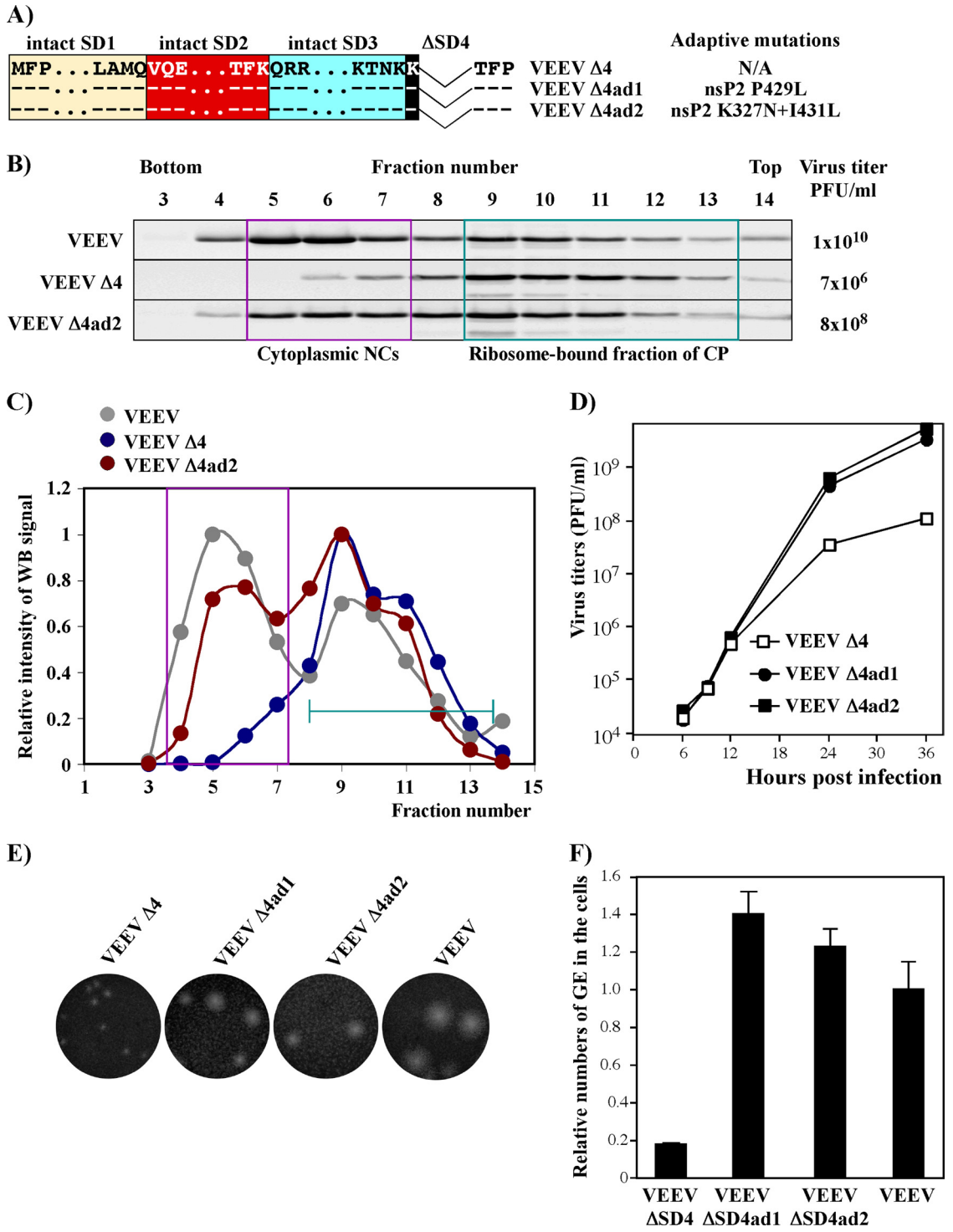

FIG 10 Adaptive mutations in nsP2 can increase infectious titers and plaque sizes of VEEV mutants with a deleted SD4 domain of the capsid protein. (A) Schematic alignment of the amino-terminal domain of capsid protein in VEEV Δ4 and the nsP2-specific compensatory mutations identified in the nsP2 gene of selected, more efficiently replicating variants. (B) Results of one of the reproducible analyses of NC and capsid protein distribution in sucrose gradients. Virus titers were determined at the time of cell harvesting at 16 h postinfection. (C) Results of quantitative analysis of the Western blot membranes presented in panel B. In each gradient, the values were normalized to the signal detected in the fraction with the highest concentration of capsid protein. Pink boxes indicate the distribution of cytoplasmic NCs. Green lines indicate positions of the ribosome-bound fraction of capsid proteins. (D) Comparative analysis of the infectious virus release by the originally designed mutant and its adapted variants, VEEV Δ4ad1 and VEEV Δ4ad2, at an MOI of 0.01 inf.u/cell. Media were replaced at the indicated times postinfection, and infectious titers were determined as described in Materials and Methods. (E) Comparative analysis of the sizes of plaques formed on BHK-21 cells by the originally designed mutant and its adapted variants. Virus stocks were titrated on BHK-21 cells as described in Materials and Methods. Plaques were stained with crystal violet after 2 days of incubation at 37°C. (F) Subconfluent BHK-21 cells in 35-mm dishes were infected with an MOI of 10 inf.u/cell. At 16 h postinfection, RNA was isolated by TRIzol and analyzed by RT-qPCR as described in Materials and Methods. The relative numbers of genome equivalents (GE) were calculated and normalized to the cellular β-actin RNA.

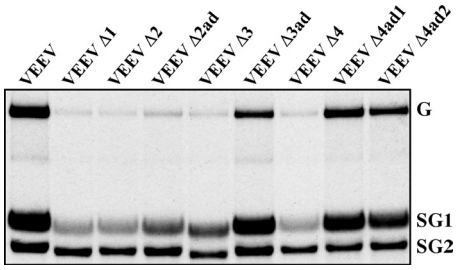

FIG 11 Deletions of SDs in VEEV capsid protein affect viral RNA synthesis, which can be restored through a number of compensatory mutations. Subconfluent BHK-21 cells in 35-mm dishes were infected at an MOI of 10 inf.u/cell with VEEV/GFP or mutated genome-containing particles, generated by coelectroporation with *in vitro*-synthesized helper RNAs. Viral RNAs were metabolically labeled with [^{3}H]uridine between 3 and 7 h postinfection and analyzed as described in Materials and Methods. The experiment was repeated twice with very similar results.

mains highly inefficient. Thus, other SDs appear to efficiently control the mispackaging of heterologous RNAs. SD1, SD2, and SD4 are dispensable for VLP formation but ensure that neutralization of the charge of SD3 is achieved by the viral genome only.

It has been previously suggested that alphavirus SD4 determines specificity of capsid's interaction with the PS in viral genomic RNA (38, 54). Indeed, in the absence of SD4 in capsid protein, infectious virus titers become 1,000-fold lower. However, this function of SD4 appears to be just one of the components of the mechanism that determines the specificity of RNA encapsidation. The deletions of SD1 and SD2 lead to an increase in packaging of cellular mRNA (Fig. 6E). Thus, SD1 and SD2 are not only structural components of NC but are also actively involved in the RNA genome packaging process. Moreover, our recent studies on the evolution of VEEV capsid mutants demonstrated that VEEV variants with highly mutated capsid protein acquire adaptive mutations in SD2 (helix I) (35). These mutations dramatically increased the efficiency of genome encapsidation, suggesting that SD2 functions not only in the previously proposed capsid protein dimerization but also in viral genome packaging.

Prior to the present study, the functions of SD1 were strongly underappreciated and had not been investigated. Our data suggest that, surprisingly, this peptide is critical for VEEV capsid function. This was the only SD whose deletion could not be compensated for by adaptive mutations in other SDs or nsPs. Adapted variants of VEEV Δ1, which could replicate to higher infectious titers, were not found in any of our experiments. In studies of SFV capsid protein assembly (21), this subdomain was left unmodified because the corresponding coding sequence in the subgenomic RNA contains a *cis*-acting element, the translational enhancer, which determines the translation efficiency of the latter RNA in the infected cells. In contrast to SINV and SFV, VEEV replication does not induce profound translational shutoff in infected cells, and the VEEV SD1-specific RNA sequence in the subgenomic RNA appears to either have no translational enhancer or perhaps contains an enhancer with a different mode of function (55). Based on the available data from this and other ongoing studies, we propose that SD1 organizes the amino-terminal capsid domains in the NC by forming an SD1 core. In the absence of other SDs, this function appears to no longer be required, and particles containing capsid with deleted SD1, SD2, SD3, and SD4 are efficiently formed. However, if the capsid contains other SDs, and SD3 in particular, these subdomains need to be additionally organized. Both VEEV/CmΔ1 and VEEV Δ1 were very inefficient in particle release and, in case of VEEV Δ1, we were unable to detect preformation of the intracellular NC, despite this variant encoding wt RNA-binding SD3, helix I/SD2, and SD4, which are supposed to be responsible for specific interaction of the capsid with genomic RNA. The mechanism of SD1 function is now under more detailed investigation.

It is also apparent that the amino-terminal domain of VEEV capsid is not the only domain involved in RNA encapsidation. Capsid mutants defective in RNA binding demonstrated accumulation of additional positively charged amino acids on the internal surface of the carboxy-terminal protease domain, which already has a high positive charge (Fig. 5). Thus, the protease domain is likely to also be an active player in RNA packaging. This provides a plausible explanation for the residual infectious virus particle formation observed in VEEV mutants in which the entire amino-terminal capsid domain was either deleted or contained no positively charged amino acids (30). Based on the experimental data, a fraction of the particles released from the cells infected with such mutants contained viral genomes, and the infectious titers approached 10^5 inf.u/ml.

Mutations in capsid protein induce virus evolution, which results in compensatory mutations, which improve the capsid-RNA interaction, in genes distinct from the capsid-coding gene. This effect had also been observed in our previous capsid studies (35). Some of the compensatory mutations found in both capsid- and nsP2-coding genes (Fig. 10) led to detectable increases in RNA replication and disproportionally strong increases in genomic RNA packaging and infectious virus release. Moreover, nsP2 evolution was possible only when mutated capsid retained its SD2. These results suggest that VEEV nonstructural protein nsP2 and capsid protein have complex interactions and functions and are likely to be involved in both RNA replication and encapsidation. Thus, we need to be very cautious in data interpretation, and further studies are required to dissect these complicated phenomena.

Taken together, the present study produced a number of findings, and these are summarized in Fig. 12. (i) VEEV particles can be efficiently formed directly at the plasma membrane without cytoplasmic NC preassembly. (ii) The entire amino-terminal domain of VEEV capsid protein is dispensable for particle formation and release. In its absence, the carboxy-terminal protease domain is capable of promoting efficient self-assembly and the release of genome-free VEEV VLPs, which have sizes and morphologies similar to those of the wt virions. (iii) The amino-terminal domain of VEEV capsid protein contains at least four functionally distinct subdomains. They determine RNA packaging and the specificity of packaging in particular. (iv) The highly positively charged SD3 is a negative regulator of NC and particle assembly, unless its positive charge is neutralized by bound viral genomic RNA. (v) Both SD1 and SD2 function as important regulators of RNA packaging, in addition to SD4, whose role in defining the specificity of RNA packaging has been previously described (38). They are not required for genome-free VLP formation but are critically involved in VEEV genome packaging. (vi) Our data suggest that the positively charged surface of VEEV capsid-specific protease domain and the very amino-terminal SD1 are also involved in interaction with viral RNA and play important roles in its encapsidation. (vii) VEEV capsid protein and nsP2 regulate

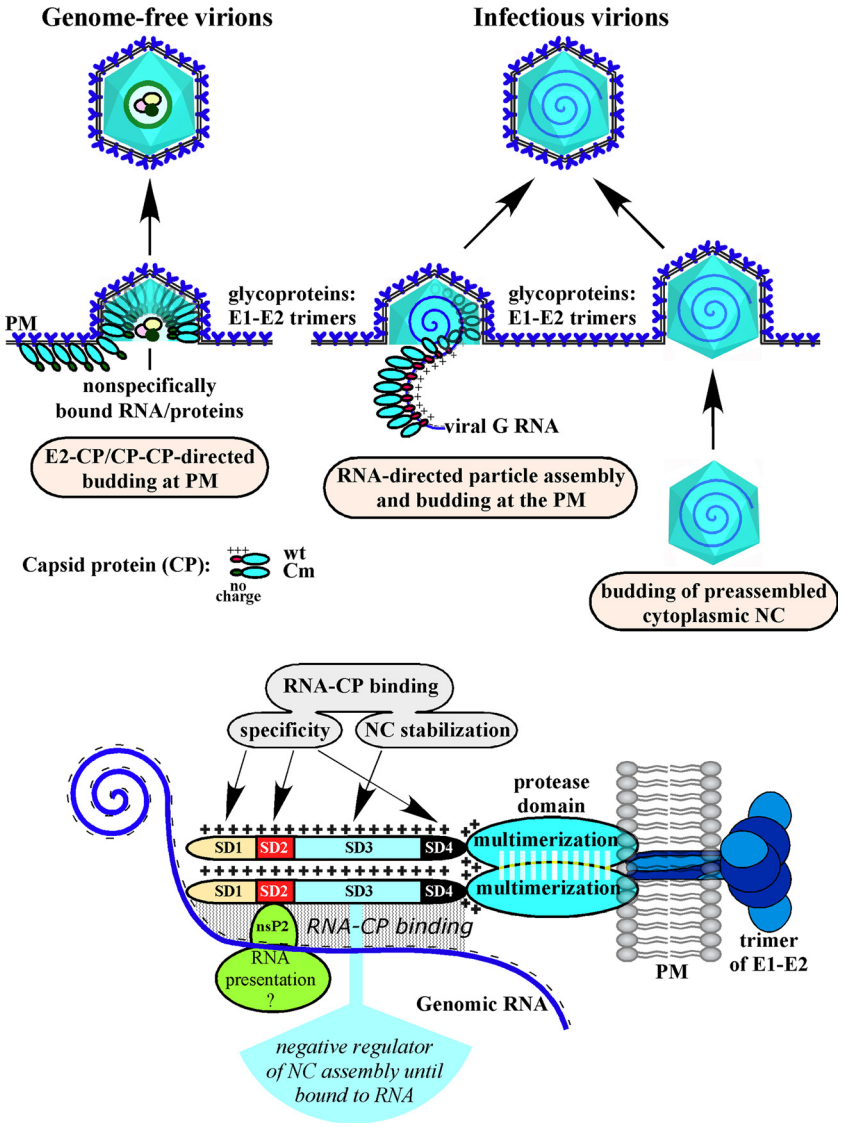

FIG 12 In cells infected with wt VEEV, the assembly of virus particles can be achieved in two different ways: (i) simultaneous NC assembly and budding at plasma membrane (PM) and (ii) budding of preformed cytoplasmic NC. The assembly of NC is regulated by RNA-CP, CP-CP, and CP-E2 interactions. RNA-CP interactions can be either specific (SD1, SD2, and SD4) or nonspecific electrostatic interactions, which function in a stabilization mode (SD3). SD3 also functions to prevent the assembly of NC until bound to viral RNA. In the absence of genomic RNA binding (by discharging the N terminus of CP), budding is directed and performed by E2-CP and CP-CP interactions.

RNA synthesis and its encapsidation, but the mechanism of these processes needs further investigation.

ACKNOWLEDGMENTS

We thank Niall J. Foy for helpful discussions, critical reading, and editing of the manuscript. We also thank Robert Tesh for providing VEEV-specific antibodies, and we thank the members of UAB cryo-EM core facility in the Center for Structural Biology for their help.

This study was supported by Public Health Service grants AI070207, AI095449, and AI093592 (I.F.) and AI073301 (E.I.F.).

REFERENCES

1. **Weaver SC, Frolov I.** 2005. Togaviruses, p 1010–1024. *In* Mahy BWJ, ter Meulen V (ed), Virology, vol 2. Hodder Arnold, Salisbury, United Kingdom.
2. **Strauss JH, Strauss EG.** 1994. The alphaviruses: gene expression, replication, evolution. Microbiol. Rev. **58:**491–562.
3. **Brown DT, Condreay LD.** 1986. Replication of alphaviruses in mosquito cells, p 171–207. *In* Schlesinger S, Schlesinger MJ (ed), The *Togaviridae* and *Flaviviridae*. Plenum Press, Inc, New York, NY.
4. **Griffin DE.** 1986. Alphavirus pathogenesis and immunity, p 209–250. *In* Schlesinger S, Schlesinger MJ (ed), The *Togaviridae* and *Flaviviridae*. Plenum Press, Inc, New York, NY.
5. **Griffin DE.** 2001. Alphaviruses, p 917–962. *In* Knipe DM, Howley PM (ed), Fields virology, 4th ed. Lippincott/The Williams & Wilkins Co, New York, NY.
6. **Dal Canto MC, Rabinowitz SG.** 1981. Central nervous system demyelination in Venezuelan equine encephalomyelitis infection. J. Neurol. Sci. **49:**397–418.
7. **Weaver SC, Ferro C, Barrera R, Boshell J, Navarro JC.** 2004. Venezuelan equine encephalitis. Annu. Rev. Entomol. **49:**141–174.
8. **Alevizatos AC, McKinney RW, Feigin RD.** 1967. Live, attenuated Venezuelan equine encephalomyelitis virus vaccine. I. Clinical effects in man. Am. J. Trop. Med. Hyg. **16:**762–768.

9. **Burke DS, Ramsburg HH, Edelman R.** 1977. Persistence in humans of antibody to subtypes of Venezuelan equine encephalomyelitis (VEE) virus after immunization with attenuated (TC-83) VEE virus vaccine. J. Infect. Dis. **136:**354–359.
10. **Pittman PR, Makuch RS, Mangiafico JA, Cannon TL, Gibbs PH, Peters CJ.** 1996. Long-term duration of detectable neutralizing antibodies after administration of live-attenuated VEE vaccine and following booster vaccination with inactivated VEE vaccine. Vaccine **14:**337–343.
11. **Kinney RM, Johnson BJB, Welch JB, Tsuchiya KR, Trent DW.** 1989. The full-length nucleotide sequences of the virulent Trinidad donkey strain of Venezuelan equine encephalitis virus and its attenuated vaccine derivative, strain TC-83. Virology **170:**19–30.
12. **Pedersen CE, Jr, Robinson DM, Cole FE, Jr.** 1972. Isolation of the vaccine strain of Venezuelan equine encephalomyelitis virus from mosquitoes in Louisiana. Am. J. Epidemiol. **95:**490–496.
13. **Akahata W, Yang ZY, Andersen H, Sun S, Holdaway HA, Kong WP, Lewis MG, Higgs S, Rossmann MG, Rao S, Nabel GJ.** 2010. A virus-like particle vaccine for epidemic Chikungunya virus protects nonhuman primates against infection. Nat. Med. **16:**334–338.
14. **Mason PW, Shustov AV, Frolov I.** 2006. Production and characterization of vaccines based on flaviviruses defective in replication. Virology **351:**432–443.
15. **Shustov AV, Mason PW, Frolov I.** 2007. Production of pseudoinfectious yellow fever virus with a two-component genome. J. Virol. **81:**11737–11748.
16. **Perera R, Navaratnarajah C, Kuhn RJ.** 2003. A heterologous coiled coil can substitute for helix I of the Sindbis virus capsid protein. J. Virol. **77:**8345–8353.
17. **Perera R, Owen KE, Tellinghuisen TL, Gorbalenya AE, Kuhn RJ.** 2001. Alphavirus nucleocapsid protein contains a putative coiled coil alpha-helix important for core assembly. J. Virol. **75:**1–10.
18. **Tellinghuisen TL, Perera R, Kuhn RJ.** 2001. In vitro assembly of Sindbis virus core-like particles from cross-linked dimers of truncated and mutant capsid proteins. J. Virol. **75:**2810–2817.
19. **Frolov I, Frolova E, Schlesinger S.** 1997. Sindbis virus replicons and Sindbis virus: assembly of chimeras and of particles deficient in virus RNA. J. Virol. **71:**2819–2829.
20. **Owen KE, Kuhn RJ.** 1997. Alphavirus budding is dependent on the interaction between the nucleocapsid and hydrophobic amino acids on the cytoplasmic domain of the E2 envelope glycoprotein. Virology **230:**187–196.
21. **Forsell K, Xing L, Kozlovska T, Cheng RH, Garoff H.** 2000. Membrane proteins organize a symmetrical virus. EMBO J. **19:**5081–5091.
22. **Forsell K, Griffiths G, Garoff H.** 1996. Preformed cytoplasmic nucleocapsids are not necessary for alphavirus budding. EMBO J. **15:**6495–6505.
23. **Forsell K, Suomalainen M, Garoff H.** 1995. Structure-function relation of the NH_2-terminal domain of the Semliki Forest virus capsid protein. J. Virol. **69:**1556–1563.
24. **Zhang R, Hryc CF, Cong Y, Liu X, Jakana J, Gorchakov R, Baker ML, Weaver SC, Chiu W.** 2011. 4.4 A cryo-EM structure of an enveloped alphavirus Venezuelan equine encephalitis virus. EMBO J. **30:**3854–3863.
25. **Strauss EG, Rice CM, Strauss JH.** 1984. Complete nucleotide sequence of the genomic RNA of Sindbis virus. Virology **133:**92–110.
26. **Frolov I, Schlesinger S.** 1994. Comparison of the effects of Sindbis virus and Sindbis virus replicons on host cell protein synthesis and cytopathogenicity in BHK cells. J. Virol. **68:**1721–1727.
27. **Jose J, Przybyla L, Edwards TJ, Perera R, Burgner JW, 2nd, Kuhn RJ.** 2012. Interactions of the cytoplasmic domain of Sindbis virus E2 with nucleocapsid cores promote alphavirus budding. J. Virol. **86:**2585–2599.
28. **Snyder JE, Berrios CJ, Edwards TJ, Jose J, Perera R, Kuhn RJ.** 2012. Probing the early temporal and spatial interaction of the Sindbis virus capsid and E2 proteins with reverse genetics. J. Virol. **86:**12372–12383.
29. **Garoff H, Sjoberg M, Cheng RH.** 2004. Budding of alphaviruses. Virus Res. **106:**103–116.
30. **Atasheva S, Kim DY, Akhrymuk M, Morgan DG, Frolova EI, Frolov I.** 2013. Pseudoinfectious Venezuelan equine encephalitis virus: a new means of alphavirus attenuation. J. Virol. **87:**2023–2035.
31. **Atasheva S, Krendelchtchikova V, Liopo A, Frolova E, Frolov I.** 2010. Interplay of acute and persistent infections caused by Venezuelan equine encephalitis virus encoding mutated capsid protein. J. Virol. **84:**10004–10015.
32. **Liljeström P, Lusa S, Huylebroeck D, Garoff H.** 1991. *In vitro* mutagenesis of a full-length cDNA clone of Semliki Forest virus: the small 6,000-molecular-weight membrane protein modulates virus release. J. Virol. **65:**4107–4113.
33. **Lemm JA, Durbin RK, Stollar V, Rice CM.** 1990. Mutations which alter the level or structure of nsP4 can affect the efficiency of Sindbis virus replication in a host-dependent manner. J. Virol. **64:**3001–3011.
34. **Gorchakov R, Frolova E, Frolov I.** 2005. Inhibition of transcription and translation in Sindbis virus-infected cells. J. Virol. **79:**9397–9409.
35. **Kim DY, Atasheva S, Frolova EI, Frolov I.** 2013. Venezuelan equine encephalitis virus nsP2 protein regulates packaging of the viral genome into infectious virions. J. Virol. **87:**4202–4213.
36. **Atasheva S, Fish A, Fornerod M, Frolova EI.** 2010. Venezuelan equine Encephalitis virus capsid protein forms a tetrameric complex with CRM1 and importin alpha/beta that obstructs nuclear pore complex function. J. Virol. **84:**4158–4171.
37. **Atasheva S, Garmashova N, Frolov I, Frolova E.** 2008. Venezuelan equine encephalitis virus capsid protein inhibits nuclear import in Mammalian but not in mosquito cells. J. Virol. **82:**4028–4041.
38. **Owen KE, Kuhn RJ.** 1996. Identification of a region in the Sindbis virus nucleocapsid protein that is involved in specificity of RNA encapsidation. J. Virol. **70:**2757–2763.
39. **Weiss B, Geigenmuller-Gnirke U, Schlesinger S.** 1994. Interactions between Sindbis virus RNAs and a 68 amino acid derivative of the viral capsid protein further defines the capsid binding site. Nucleic Acids Res. **22:**780–786.
40. **Frolov I, Schlesinger S.** 1994. Translation of Sindbis virus mRNA: effects of sequences downstream of the initiating codon. J. Virol. **68:**8111–8117.
41. **Frolov I, Schlesinger S.** 1996. Translation of Sindbis virus mRNA: analysis of sequences downstream of the initiating AUG codon that enhance translation. J. Virol. **70:**1182–1190.
42. **Berglund P, Tubulekas I, Liljestrom P.** 1996. Alphaviruses as vectors for gene delivery. Trends Biotechnol. **14:**130–134.
43. **Garmashova N, Atasheva S, Kang W, Weaver SC, Frolova E, Frolov I.** 2007. Analysis of Venezuelan equine encephalitis virus capsid protein function in the inhibition of cellular transcription. J. Virol. **81:**13552–13565.
44. **Garmashova N, Gorchakov R, Volkova E, Paessler S, Frolova E, Frolov I.** 2007. The Old World and New World alphaviruses use different virus-specific proteins for induction of transcriptional shutoff. J. Virol. **81:**2472–2484.
45. **Voss JE, Vaney MC, Duquerroy S, Vonrhein C, Girard-Blanc C, Crublet E, Thompson A, Bricogne G, Rey FA.** 2010. Glycoprotein organization of Chikungunya virus particles revealed by X-ray crystallography. Nature **468:**709–712.
46. **Li L, Jose J, Xiang Y, Kuhn RJ, Rossmann MG.** 2010. Structural changes of envelope proteins during alphavirus fusion. Nature **468:**705–708.
47. **Froshauer S, Kartenbeck J, Helenius A.** 1988. Alphavirus RNA replicase is located on the cytoplasmic surface of endosomes and lysosomes. J. Cell Biol. **107:**2075–2086.
48. **Snyder JE, Azizgolshani O, Wu B, He Y, Lee AC, Jose J, Suter DM, Knobler CM, Gelbart WM, Kuhn RJ.** 2011. Rescue of infectious particles from preassembled alphavirus nucleocapsid cores. J. Virol. **85:**5773–5781.
49. **Frolova E, Gorchakov R, Garmashova N, Atasheva S, Vergara LA, Frolov I.** 2006. Formation of nsP3-specific protein complexes during Sindbis virus replication. J. Virol. **80:**4122–4134.
50. **Frolova EI, Gorchakov R, Pereboeva L, Atasheva S, Frolov I.** 2010. Functional Sindbis virus replicative complexes are formed at the plasma membrane. J. Virol. **84:**11679–11695.
51. **Gorchakov R, Garmashova N, Frolova E, Frolov I.** 2008. Different types of nsP3-containing protein complexes in Sindbis virus-infected cells. J. Virol. **82:**10088–10101.
52. **Suomalainen M, Liljestrom P, Garoff H.** 1992. Spike protein-nucleocapsid interactions drive the budding of alphaviruses. J. Virol. **66:**4737–4747.
53. **Zheng Y, Kielian M.** 2013. Imaging of the alphavirus capsid protein during virus replication. J. Virol. **87:**9579–9889.
54. **Kim DY, Firth AE, Atasheva S, Frolova EI, Frolov I.** 2011. Conservation of a packaging signal and the viral genome RNA packaging mechanism in alphavirus evolution. J. Virol. **85:**8022–8036.
55. **Volkova E, Frolova E, Darwin JR, Forrester NL, Weaver SC, Frolov I.** 2008. IRES-dependent replication of Venezuelan equine encephalitis virus makes it highly attenuated and incapable of replicating in mosquito cells. Virology **377:**160–169.